

Magnetohydrodynamic Wave Propagation from a Localized Source Including Hall Effect

E. G. Broadbent

Phil. Trans. R. Soc. Lond. A 1968 **263**, 119-147

doi: 10.1098/rsta.1968.0008

Email alerting service

Receive free email alerts when new articles cite this article - sign up in the box at the top right-hand corner of the article or click [here](#)

To subscribe to *Phil. Trans. R. Soc. Lond. A* go to: <http://rsta.royalsocietypublishing.org/subscriptions>

MAGNETOHYDRODYNAMIC WAVE PROPAGATION FROM A LOCALIZED SOURCE INCLUDING HALL EFFECT

By E. G. BROADBENT

Royal Aircraft Establishment, Farnborough, Hants

(Communicated by D. Küchemann, F.R.S.—Received 5 October 1967)

CONTENTS

	PAGE		PAGE
1. INTRODUCTION	119	3. TWO-FLUID TREATMENT	136
2. M.H.D. TREATMENT INCLUDING HALL CURRENT	121	3.1. Derivation of the wave number surface	136
2.1. Typical laboratory plasma	121	3.2. Electron inertia and electron forcing functions	139
2.2. Derivation of the wave number surface	122	4. AN EFFECT OF COLLISIONS (FINITE ELECTRICAL CONDUCTIVITY)	140
2.3. Wave propagation at very low frequency	125	5. CONCLUSIONS	144
2.4. Wave propagation at frequencies of the order of the ion cyclotron frequency	128	APPENDIX	144
2.5. The effect of a doublet disturbance at the origin	134	PRINCIPAL SYMBOLS	146
		REFERENCES	147

Lighthill's theorem on magnetohydrodynamic wave propagation from a localized source gives an asymptotic expression for the wave amplitude at large distance from the source and this theorem is applied to a laboratory plasma. Attention is focused mainly on conditions where the Alfvén speed is large compared with the sound speed and where the wave frequency is of the same order as the ion cyclotron frequency. These conditions are also typical of certain natural plasmas. The manner in which the wave amplitude depends on the direction of propagation and on the ratio of the wave frequency to the ion cyclotron frequency is examined and illustrated by graphs which also cover a range of source sizes. An extension is made into a two-fluid theory such that electron inertia and electron source terms can be included and the effect of finite electrical conductivity is considered.

1. INTRODUCTION

In 1961 suggestions were made (Broadbent 1961) for setting up a low temperature laboratory plasma in potassium vapour with a view to investigating the propagation of acoustic waves. These tentative ideas have now been developed into a detailed set of proposed experiments with fairly precise values of plasma temperature and density, magnetic field strength, frequency, etc. (Knight 1965) and it seems appropriate to examine more closely the expected behaviour of acoustic waves diverging from a source in such conditions. The theory is given by Lighthill (1960), who considers the propagation of waves from a source of length scale l in the far field, such that the distance r from the source region is large compared with l . This theory assumes that the electrical resistance of the plasma is negligible, i.e. that the ion-

electron collision frequency is small compared with the applied frequency. Lighthill (1960) applies the theory in two examples,

(1) where the speed of sound a_0 , given by $\partial p/\partial \rho$ at constant entropy (p and ρ are gas pressure and density respectively) is finite, as also is the Alfvén speed a_1 given by $B_0/(\mu\rho)^{\frac{1}{2}}$ where B_0 is the steady magnetic field strength, and μ the magnetic permeability.† In this application a single perfectly conducting fluid is assumed such that the magnetic field lines are frozen into the gas;

(2) the speed of sound is put infinite ($a_0/a_1 \gg 1$) but Hall current is permitted to flow and the magnetic field is frozen into the electron gas.

In example (1) it was found that if $a_0 > a_1$ a sound-like wave propagates outwards from a source with the shape of a distorted sphere while a mainly hydromagnetic wave propagates within a narrow cone whose axis lies along the magnetic field. This, at least, is true of disturbances like $\text{div } \mathbf{v}$ ($\equiv \Delta$) which is of main interest in sound-like waves (\mathbf{v} is the local fluid velocity), or $\partial v_x/\partial x$ ($\equiv \Gamma$), where x is the direction of \mathbf{B}_0 , but Lighthill shows also that the x -component of vorticity propagates without attenuation in the x -direction. If, in example (1), $a_1 > a_0$, the rôles of the two types of wave are reversed and it is the sound-like wave that propagates within the cone; this is in fact the state of affairs to be expected in the laboratory. The second example shows that the two remaining variables (since $\text{div } \mathbf{v} = 0$ when $a_0 \rightarrow \infty$) again propagate within a cone whose axis lies along the magnetic field. One of the main features of the proposed experiments is to test this conical propagation.

In § 2 of the present paper Lighthill's results are extended to cover the case where Hall current is included and both a_0 and a_1 are finite, although the limit $a_1/a_0 \rightarrow \infty$ is of particular interest. The Hall effect is found to lead to conical wave propagation at frequencies below the ion cyclotron frequency, and the amplitude distribution is examined both for a pure source and a doublet. These results are deduced from a wave number surface, with the aid of a theorem due to Lighthill (1960), and in § 3 this surface is obtained by a different method keeping separate equations for the ion gas and the electron gas and applying matrix algebra in a manner akin to that used, for example, by Allis, Buchsbaum & Bers (1963). This method has the advantage that it is rather easier to include additional effects such as, for example, terms of order electron mass compared with those of ion mass. Such terms are small, but in the proposed experiments are no smaller than the second-order terms in a_0/a_1 (since it is the square of this ratio that matters) and could be of interest near singularities like $\omega/\omega_i \rightarrow 1$, where ω is the applied frequency and ω_i the ion cyclotron frequency. These terms are considered in § 3, and in § 4 the effects of finite conductivity are examined.

In the laboratory the origin of the disturbance will be an applied alternating electric field and it is a separate issue whether a reasonable proportion of the electric energy supplied in this way is converted into mechanical acoustic energy, for the ion acoustic waves carry negligible electric energy. This question has been examined and will be reported separately, but it appears that adequate acoustic excitation can be achieved within a reasonable distance of the source. Some confirmation of this is found in the present paper (§ 3), where sources and doublets in the electron gas only are considered.

† SI units are used throughout the present paper.

2. M.H.D. TREATMENT INCLUDING HALL CURRENT

2.1. *Typical laboratory plasma*

Knight (1965) gives typical plasma properties as:

temperature T	2300 °K
electron density n_e	$2.8 \times 10^{19} \text{ m}^{-3}$
sound speed a_0	$1.14 \times 10^3 \text{ m s}^{-1}$
frequency $\omega/2\pi$	$1.95 \times 10^5 \text{ Hz}$
ion collision time τ_{ii}	$0.196 \times 2\pi/\omega \text{ s}$
magnetic field B_0	0.5 Wb m^{-2}

These figures relate to ionized potassium vapour. The sound speed is the plasma sound speed given by

$$a_0 = \frac{\omega}{k} = \left\{ \frac{k_B(\gamma_e T_e + \gamma_i T_i)}{m_e + m_i} \right\}^{\frac{1}{2}}, \quad (1)$$

where

\mathbf{k} is the wave number vector,

γ is the ratio of specific heats,

m is the particle mass,

k_B is Boltzmann's constant ($1.38 \times 10^{-23} \text{ J}^\circ\text{K}^{-1}$) and suffix i relates to ions and e to electrons. Numerical values of the masses are:

$$m_e = 9.113 \times 10^{-31} \text{ kg}$$

$$m_i (\text{potassium}) = 6.5 \times 10^{-26} \text{ kg} = 7.13 \times 10^4 m_e.$$

The numerical evaluation of a_0 in (1) depends on the choice of γ_i and γ_e , and in obtaining the speed of 1140 m s^{-1} Knight argued first, that the number of ion collisions per cycle (about 5) was sufficient for γ_i to have its fully relaxed value of $\gamma_i = \frac{5}{3}$, and secondly, that the electron motion is so rapid compared with the applied frequency that it is effectively isothermal giving $\gamma_e = 1$. The ion and electron temperatures are taken to be equal, so that this is equivalent to taking a mean γ of $\frac{4}{3}$. Equation (1) also illustrates the fact that the sound speed is almost exactly $\sqrt{2}$ times what it would be for a neutral gas at the same temperature, molecular weight and mean γ , since the electrons contribute pressure but negligible mass.

With regard to frequencies, the parameter ω is used throughout the present paper as an angular frequency, e.g. as in $e^{i\omega t}$, so that frequencies in hertz are indicated by writing $\omega/2\pi$. The ion cyclotron frequency is given by

$$\begin{aligned} \omega_i &= eB_0/m_i \\ &= 1.23 \times 10^6 \text{ s}^{-1} \quad \text{for } B_0 = 0.5 \text{ Wb m}^{-2} \quad (\omega_i/2\pi = 1.96 \times 10^5 \text{ Hz}). \end{aligned} \quad (2)$$

Other frequencies of possible interest are the plasma frequency ω_p and the electron cyclotron frequency ω_e ; these have typical values given by

$$\left. \begin{aligned} \omega_p &= (n_e e^2 / \epsilon m_e)^{\frac{1}{2}} \\ &= 3 \times 10^{11} \text{ s}^{-1} \quad (\omega_p/2\pi = 4.75 \times 10^{10} \text{ Hz}), \\ \omega_e &= eB/m_e \\ &= 8.8 \times 10^{10} \text{ s}^{-1} \quad (\omega_e/2\pi = 1.4 \times 10^{10} \text{ Hz}). \end{aligned} \right\} \quad (3)$$

The Alfvén speed a_1 is given by

$$a_1 = B_0 / \sqrt{(\mu\rho)} = 3.31 \times 10^5 \text{ m s}^{-1}.$$

Thus $(a_1/a_0)^2 = 8.43 \times 10^4$ is the same order as m_i/m_e .

These conditions will be used as the basis of the subsequent theoretical applications, since it is desirable to have a specific aim in mind when considering wave propagation in a plasma because of the very wide range of possible phenomena. They are, however, typical of both the ionosphere and the upper regions of the Sun's atmosphere for certain frequencies and wavelengths. One prerequisite is that the plasma shall be collision dominated or that $\omega\tau_{ii} < 1$ (Knight 1965; Neubert 1966; Frood 1963). In the ionosphere at 330 km altitude (day time) where τ_{ii} is about $\frac{1}{2}$ s this implies $\omega < 1 \text{ s}^{-1}$ approximately which is much below the ion cyclotron frequency of about 600 s^{-1} . The sound speed is about 10^3 m s^{-1} and the Alfvén speed about $5 \times 10^5 \text{ m s}^{-1}$ if the neutrals are not disturbed or about 10^4 m s^{-1} if they participate in the motion. On this last point the neutral mean free path is about 1.3 km and the ion mean free path about 0.65 km so that the extent to which the neutrals participate will depend on the wavelength.

In the Sun's atmosphere typical figures near a sunspot in the chromosphere would be:

$$T = 6 \times 10^3 \text{ }^\circ\text{K}; n_a = 10^{20} \text{ m}^{-3}; n_e = 10^{18} \text{ m}^{-3}; \text{ atomic free path } 9 \times 10^{-2} \text{ m}; \text{ ion free path } 2 \times 10^{-2} \text{ m}; \text{ sound speed } 9 \times 10^3 \text{ m s}^{-1}; \text{ Alfvén speed (including neutral gas inertia) } 2 \times 10^5 \text{ m s}^{-1} \text{ for a magnetic field of } 0.1 \text{ tesla}; \tau_{ii} = 2 \times 10^{-6} \text{ s}; \omega_i = 10^7 \text{ s}^{-1}.$$

The subsequent analysis should thus also apply to such regions of the Sun's atmosphere.

2.2. Derivation of the wave number surface

Lighthill (1960) gives the asymptotic solution for large \mathbf{r} to the equation

$$P\left(\frac{\partial^2}{\partial t^2}, \frac{\partial^2}{\partial x^2}, \frac{\partial^2}{\partial y^2}, \frac{\partial^2}{\partial z^2}\right)u = e^{i\omega t}f(x, y, z), \quad (4)$$

where the left-hand side is a polynomial of the second-order derivatives in space and time of a fluid disturbance u , and the right-hand side is a forcing function such that f vanishes outside a restricted region. The polynomial P is determined by the physics of the medium, and will be derived here since it contains terms additional to those given by Lighthill. The electron and ion momentum equations are (in Lighthill's notation)

$$n_e m_e \left(\frac{\partial \mathbf{v}_e}{\partial t} + \mathbf{v}_e \cdot \nabla \mathbf{v}_e \right) = -\nabla p_e - \mathbf{M} - n_e e (\mathbf{E} + \mathbf{v}_e \wedge \mathbf{B}), \quad (5)$$

$$n_i m_i \left(\frac{\partial \mathbf{v}_i}{\partial t} + \mathbf{v}_i \cdot \nabla \mathbf{v}_i \right) = -\nabla p_i + \mathbf{M} + n_i e (\mathbf{E} + \mathbf{v}_i \wedge \mathbf{B}), \quad (6)$$

where p is pressure, \mathbf{E} is electric field and \mathbf{M} is rate of electron momentum loss through ion collision which can be written

$$\mathbf{M} = -n_e e \eta \mathbf{j} \quad (7)$$

and η is the electrical resistivity, with \mathbf{j} the electric current density.

To get the equation of plasma momentum, (5) and (6) are added with $n_e = n_i$ and with

$$n_i e \mathbf{v}_i - n_e e \mathbf{v}_e = \mathbf{j} = \frac{\text{curl } \mathbf{B}}{\mu} \quad (8)$$

this gives (for negligible m_e/m_i)

$$\rho \left(\frac{\partial \mathbf{v}}{\partial t} + \mathbf{v} \cdot \nabla \mathbf{v} \right) = -\nabla p + \frac{1}{\mu} (\text{curl } \mathbf{B}) \wedge \mathbf{B} \quad (9)$$

where, in (8), the displacement current is neglected. In equation (5) the left-hand side is of order m_e/m_i compared with the right and if we neglect this and the resistance term M an equation for \mathbf{E} is obtained

$$\mathbf{E} = - \left(\frac{\nabla p_e}{en_e} + \mathbf{v}_e \wedge \mathbf{B} \right). \quad (10)$$

Maxwell's equation now gives

$$\begin{aligned} \frac{\partial \mathbf{B}}{\partial t} &= -\text{curl } \mathbf{E} \\ &= \text{curl} (\mathbf{v}_e \wedge \mathbf{B}), \\ \frac{\partial \mathbf{B}}{\partial t} &= \text{curl} \left\{ \left(\mathbf{v} - \frac{\text{curl } \mathbf{B}}{\mu n_e e} \right) \wedge \mathbf{B} \right\}, \end{aligned} \quad (11)$$

if we use (8), assume $\mathbf{v}_i \simeq \mathbf{v}$ and neglect $\text{curl} \{ \nabla p_e / n_e \}$ as in Lighthill (1960) (n_e is a direct function of p_e , and nearly proportional to it at the low frequencies appropriate to ion waves).

Equations (8) and (11) for plasma momentum and magnetic field, together with the continuity equation and adiabatic equation (without dissipation)

$$\left. \begin{aligned} \frac{\partial \rho}{\partial t} + \text{div}(\rho \mathbf{v}) &= 0, \\ \frac{\partial p}{\partial t} + \mathbf{v} \cdot \nabla p &= a^2 \left(\frac{\partial \rho}{\partial t} + \mathbf{v} \cdot \nabla \rho \right) \end{aligned} \right\} \quad (12)$$

complete the system. The equations are linearized for small disturbances to give

$$\frac{\partial \mathbf{v}}{\partial t} = -\frac{1}{\rho_0} \nabla p + \frac{1}{\mu \rho_0} (\text{curl } \mathbf{B}) \wedge \mathbf{B}_0, \quad (13)$$

$$\frac{\partial \mathbf{B}}{\partial t} = \text{curl} (\mathbf{v} \wedge \mathbf{B}_0) - \frac{m_i}{\mu e \rho_0} (\mathbf{B}_0 \cdot \nabla) \text{curl } \mathbf{B}, \quad (14)$$

$$\frac{\partial \rho}{\partial t} = -\rho_0 \text{div } \mathbf{v}, \quad (15)$$

$$\frac{\partial p}{\partial t} = a_0^2 \frac{\partial \rho}{\partial t}. \quad (16)$$

The two applications given by Lighthill use these equations (i) with the last term in (14) neglected and (ii) with that term included but with (15) equated to zero. To eliminate unwanted variables it is convenient to write (13) and (14) with \mathbf{B}_0 in the x direction, whence

$$\frac{\partial \mathbf{v}}{\partial t} = -\frac{1}{\rho_0} \nabla p + \frac{B_0}{\mu \rho_0} (\text{curl } \mathbf{B}) \wedge \mathbf{i}, \quad (17)$$

$$\frac{\partial \mathbf{B}}{\partial t} = B_0 \text{curl} (\mathbf{v} \wedge \mathbf{i}) - \frac{m_i B_0}{\mu e \rho_0} \frac{\partial}{\partial x} \text{curl } \mathbf{B}, \quad (18)$$

where \mathbf{i} is a unit vector in the x direction. The curl of (17) gives

$$\frac{\partial}{\partial t} \text{curl } \mathbf{v} = \frac{B_0}{\mu\rho_0} \frac{\partial}{\partial x} \text{curl } \mathbf{B}. \quad (19)$$

The variable \mathbf{B} can now be eliminated by expressing $\partial\mathbf{B}/\partial t$ in terms of \mathbf{v} from (18) and (19), taking the curl of the result and substituting in the equation for $\partial^2\mathbf{v}/\partial t^2$ from (17). The pressure gradient is then removed by use of (15) and (16) to get an equation for \mathbf{v} which may be written in component form, with $\mathbf{v} = (u, v, w)$ as

$$-\frac{\partial^2 u}{\partial t^2} + a_0^2 \frac{\partial}{\partial x} \text{div } \mathbf{v} = 0, \quad (20)$$

$$\left(-\frac{\partial^2}{\partial t^2} + a_1^2 \frac{\partial^2}{\partial x^2}\right) v + \frac{m_i B_0}{e\mu\rho_0} \frac{\partial}{\partial t} \nabla^2 w = -a_0^2 \frac{\partial}{\partial y} \text{div } \mathbf{v} - a_1^2 \frac{\partial}{\partial y} \text{div } \mathbf{v} + a_1^2 \frac{\partial^2 u}{\partial x \partial y} + \frac{m_i B_0}{e\mu\rho_0} \frac{\partial}{\partial t} \frac{\partial}{\partial z} \text{div } \mathbf{v}, \quad (21)$$

$$\left(-\frac{\partial^2}{\partial t^2} + a_1^2 \frac{\partial^2}{\partial x^2}\right) w - \frac{m_i B_0}{e\mu\rho_0} \frac{\partial}{\partial t} \nabla^2 v = -a_0^2 \frac{\partial}{\partial z} \text{div } \mathbf{v} - a_1^2 \frac{\partial}{\partial z} \text{div } \mathbf{v} + a_1^2 \frac{\partial^2 u}{\partial x \partial z} - \frac{m_i B_0}{e\mu\rho_0} \frac{\partial}{\partial t} \frac{\partial}{\partial y} \text{div } \mathbf{v}. \quad (22)$$

A single equation for $\text{div } \mathbf{v}$ can be obtained by eliminating v and w separately from (21) and (22), noting that $\partial v/\partial y + \partial w/\partial z = \text{div } \mathbf{v} - \partial u/\partial x$, and after performing this addition substituting for u from (20). There results, with $\text{div } \mathbf{v} \equiv \Delta$

$$\begin{aligned} & \left(\frac{\partial^4}{\partial t^4} - 2a_1^2 \frac{\partial^4}{\partial t^2 \partial x^2}\right) \left(\frac{\partial^2}{\partial t^2} - a_0^2 \frac{\partial^2}{\partial x^2}\right) \Delta + a_1^4 \frac{\partial^4}{\partial x^4} \frac{\partial^2}{\partial t^2} \Delta + \frac{m_i^2}{e^2 \mu\rho_0} a_1^2 \frac{\partial^2}{\partial t^2} \nabla^4 \left(\frac{\partial^2}{\partial t^2} - a_0^2 \frac{\partial^2}{\partial x^2}\right) \Delta \\ & - (a_0^2 + a_1^2) \left(\frac{\partial^2}{\partial t^2} - a_1^2 \frac{\partial^2}{\partial x^2}\right) \left(\frac{\partial^2}{\partial y^2} + \frac{\partial^2}{\partial z^2}\right) \frac{\partial^2 \Delta}{\partial t^2} + a_0^2 a_1^2 \frac{\partial^2}{\partial t^2} \left(\frac{\partial^2}{\partial y^2} + \frac{\partial^2}{\partial z^2}\right) \frac{\partial^2 \Delta}{\partial x^2} \\ & - a_1^4 a_0^2 \frac{\partial^4}{\partial x^4} \nabla^2 \Delta - \frac{m_i^2 a_1^2}{e^2 \mu\rho_0} \frac{\partial^4}{\partial t^4} \nabla^2 \left(\frac{\partial^2}{\partial y^2} + \frac{\partial^2}{\partial z^2}\right) \Delta = 0. \quad (23) \end{aligned}$$

Equation (23) is also satisfied by u and hence by Γ ; it is now equivalent to (4) with zero right-hand side (forcing functions will be considered later) and the polynomial

$$P\left(\frac{\partial^2}{\partial t^2}, \frac{\partial^2}{\partial x^2}, \frac{\partial^2}{\partial y^2}, \frac{\partial^2}{\partial z^2}\right) \Delta$$

is given by the left-hand side. Following Lighthill (1960) we let

$$G = P(-\omega^2, -k_1^2, -k_2^2, -k_3^2) \quad (24)$$

where $\mathbf{k} = (k_1, k_2, k_3)$.

Since

$$\frac{m_i^2}{e^2 \mu\rho_0} = \left(\frac{m_i^2}{e^2 B_0^2}\right) \left(\frac{B_0^2}{\mu\rho_0}\right) = \frac{a_1^2}{\omega_i^2}$$

there follows

$$\begin{aligned} G \equiv & -(\omega^4 - 2a_1^2 \omega^2 k_1^2) (\omega^2 - a_0^2 k_1^2) - a_1^4 k_1^4 \omega^2 + (\omega/\omega_i)^2 a_1^4 k_1^4 (\omega^2 - a_0^2 k_1^2) \\ & + (a_0^2 + a_1^2) (\omega^2 - a_1^2 k_1^2) (k^2 - k_1^2) \omega^2 - a_0^2 a_1^2 \omega^2 k_1^2 (k^2 - k_1^2) + a_1^4 a_0^2 k_1^4 k^2 \\ & - (a_1^4 \omega^4 / \omega_i^2) k^2 (k^2 - k_1^2). \quad (25) \end{aligned}$$

In the laboratory $a_1 \gg a_0$, so we let

$$\epsilon = a_0^2/a_1^2 \quad (26)$$

and introduce

$$\left. \begin{aligned} \alpha^2 &= k_1^2 a_0^2/\omega^2, \\ \theta^2 &= (k^2 - k_1^2) a_0^2/\omega^2 \end{aligned} \right\} \quad (27)$$

and

$$\chi = (\omega/\omega_i)^2,$$

so that α here can be identified with the non-dimensional form of α used by Lighthill (1960) in his wave number diagrams† and θ^2 with Lighthill's non-dimensional form of $\beta^2 + \gamma^2$. Equation (25) may now be written

$$\left(\frac{a_0}{\omega a_1}\right)^6 G \equiv -\epsilon^3(1 - \alpha^2 - \theta^2) + \epsilon^2\{(1 - \alpha^2)(2\alpha^2 + \theta^2) - \alpha^2\theta^2\} \\ + \epsilon\alpha^2\{\alpha^2(\alpha^2 + \theta^2) - \alpha^2 - \theta^2 + \chi(\alpha^2 + \theta^2)(1 - \alpha^2 - \theta^2)\} \quad (28)$$

and the wave number surface is given by $G = 0$. As a check we note that when $\chi \rightarrow 0$ the expression (28) factorizes into $(\alpha^2 - \epsilon)$ times a factor which is proportional to the expression given by Lighthill (1960) in equation (82). A further check is provided by letting $a_0 \rightarrow \infty$ when (28) may be reduced to Lighthill's (112) times a factor.

2.3. Wave propagation at very low frequency

This is the condition examined by Lighthill (1960) in which $\chi \rightarrow 0$ and (28) becomes

$$\left(\frac{a_0}{\omega a_1}\right)^6 G \equiv \epsilon(\alpha^2 - \epsilon) [(\alpha^2 + \theta^2)(\alpha^2 - 1) + \epsilon\{1 - (\alpha^2 + \theta^2)\}]. \quad (29)$$

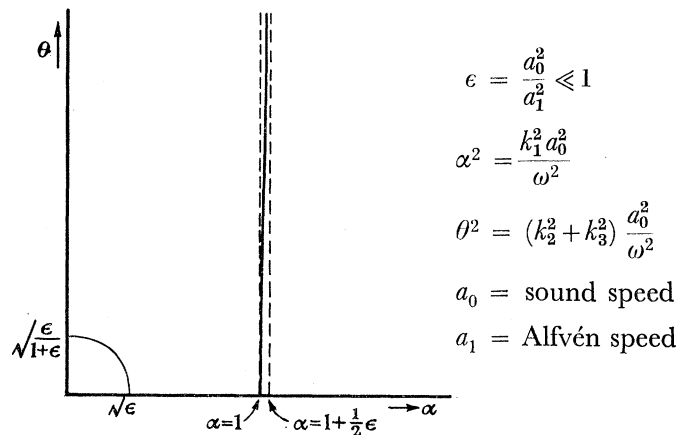


FIGURE 1. Low frequency wave number surface (full lines) for sound speed small compared with Alfvén speed.

A wave number surface is defined by the vanishing of the expression in square brackets in (29) and is illustrated in figure 1. For small ϵ a nearly plane surface is found near $\alpha = 1$ and lying wholly between $\alpha = 1$, where it intersects the axis $\theta = 0$, and $\alpha = \sqrt{1 + \epsilon}$ which it approaches asymptotically as $\theta \rightarrow \infty$. In addition there is a small nearly spherical surface near the origin bounded by $\alpha = \pm\sqrt{\epsilon}$ and $\theta = \pm\sqrt{\{\epsilon/(1 + \epsilon)\}}$.

† It is also necessary to interchange a_0 and a_1 , as mentioned by Lighthill since here $a_1 > a_0$.

The value of these wave number surfaces in discussing wave propagation follows from Lighthill's theorem 2 (1960) which says that the solution of (4) which satisfies the radiation condition, is asymptotically

$$u = \frac{4\pi^2 e^{i\omega t}}{r} \Sigma \frac{CF \exp\{i(k_1 x + k_2 y + k_3 z)\}}{|\nabla G| \sqrt{|K|}} + O\left(\frac{1}{r^2}\right) \quad (30)$$

as $r \rightarrow \infty$ along any radius vector l if the sum Σ is over all points (k_1, k_2, k_3) of the surface $G = 0$ where the normal to the surface is parallel to l and

$$\frac{\mathbf{r} \cdot \nabla G}{\partial G / \partial \omega} > 0; \quad (31)$$

provided that the surface has non-zero Gaussian curvature K at each of these points; that C is (i) $\pm i$ where $K < 0$ and ∇G is in the direction of $\pm r$, (ii) ± 1 where $K > 0$ and the surface is convex to the direction of $\pm \nabla G$; that

$$F(k_1, k_2, k_3) = \frac{1}{8\pi^3} \int_{-\infty}^{\infty} \int_{-\infty}^{\infty} \int_{-\infty}^{\infty} f(x, y, z) \exp\{-i(k_1 x + k_2 y + k_3 z)\} dx dy dz \quad (32)$$

and where G has the form (24).

Here condition (31) is the radiation condition which says that the group velocity of the waves,

$$u_g = \frac{\nabla G}{\partial G / \partial \omega} \quad (33)$$

must be directed away from the source which is in the region near $r = 0$. In the present example G is reducible to a quartic in ω which may be written

$$G_1 = \frac{a_1^2 \omega^4}{a_0^2} [(\alpha^2 + \theta^2)(\alpha^2 - 1) + \epsilon\{1 - (\alpha^2 + \theta^2)\}]. \quad (34)$$

The corresponding expression (Lighthill 1960) for the forcing function due to a point source $q e^{i\omega t} \delta(x) \delta(y) \delta(z)$ on the right-hand side of (15) is for the disturbance Γ

$$f = \frac{a_0^2 q}{\rho_0} \left\{ \frac{\partial^2}{\partial x^2} (a_1^2 \nabla^2 + \omega^2) \delta(x) \delta(y) \delta(z) \right\} \quad (35)$$

and using (32)

$$F = \frac{1}{8\pi^3} \frac{a_0^2 q}{\rho_0} k_1^2 \omega^2 \left\{ -1 + \frac{a_1^2 k^2}{\omega^2} \right\}. \quad (36)$$

These point source results may be regarded as the limit as the length scale $l \rightarrow 0$ of a source

$$q e^{i\omega t} \left[\frac{\exp\{-(x^2 + y^2 + z^2)/l^2\}}{(l\sqrt{\pi})^3} \right] \quad (37)$$

when the factor in square brackets replaces $\delta(x) \delta(y) \delta(z)$ in equation (35) and leads to an additional factor $\exp(-\frac{1}{4}k^2 l^2)$ on the right-hand side of (36). On the wave number surface G_1 vanishes and F can be written

$$F = -\frac{q\omega^4 \alpha^2 (\alpha^2 - \epsilon)}{8\pi^3 \rho_0 (\alpha^2 - 1 - \epsilon)}. \quad (38)$$

Lighthill's theorem now leads to the result that the near-sound waves propagate only within a cone whose semi-angle is equal to the range of the slope of the near-plane surface

of figure 1 which for small ϵ approximates (Lighthill 1960) to 18.6ϵ degrees of angle. In the laboratory

$$\left. \begin{aligned} \epsilon &= (a_0/a_1)^2 = 1.19 \times 10^{-5}, \\ \text{semi-cone angle} &= 2.2 \times 10^{-4} \text{ degrees.} \end{aligned} \right\} \quad (39)$$

The magnetohydrodynamic waves propagate in all directions but if \mathcal{E}_s is the energy propagated in the near-sound wave and \mathcal{E}_m in the m.h.d. wave, then

$$\frac{\mathcal{E}_s}{\mathcal{E}_m} = \left(\frac{u_s}{u_m} \right)^2. \quad (40)$$

This implies that if a non-singular direction is chosen in which each branch of the wave number surface has a single real normal, then by (30)

$$\frac{\mathcal{E}_s}{\mathcal{E}_m} = \left\{ \frac{F^2}{(\nabla G)^2 |K|} \right\}_s \left\{ \frac{(\nabla G)^2 |K|}{F^2} \right\}_m. \quad (41)$$

Of the various ratios on the right of (41) we can see that the ratio F_s^2/F_m^2 will be given by (38) with α near unity for F_s and of order $\sqrt{\epsilon}$ for F_m . Thus in the laboratory

$$\left(\frac{F_s}{F_m} \right)^2 = O\left(\frac{1}{\epsilon^6}\right). \quad (42)$$

The other factors that enter equation (41) can be estimated from the expression given by Lighthill for K and $|\nabla G|$, and here the appropriate form is that in which G is a function of α^2 and θ^2 . Let

$$\left. \begin{aligned} \alpha^2 &= A, \\ \theta^2 &= B. \end{aligned} \right\} \quad (43)$$

Then

$$\left. \begin{aligned} K &= \frac{G_B \{ 2AB(G_{AA}G_B^2 - 2G_{AB}G_A G_B + G_{BB}G_A^2) + G_A G_B (AG_A + BG_B) \}}{(AG_A^2 + BG_B^2)^2}, \\ |\nabla G| &= 2(AG_A^2 + BG_B^2)^{\frac{1}{2}}, \end{aligned} \right\} \quad (44)$$

where suffices denote partial differentiation. Using (34) the ratio $\{(\nabla G)^2 |K|\}_s / \{(\nabla G)^2 |K|\}_m$ is found to be of order ϵ^2 whence

$$\mathcal{E}_m / \mathcal{E}_s = O(\epsilon^8) \quad (45)$$

which is of order 10^{-40} in the laboratory experiment.

The result (45) applies to the energy of the wave only in so far as it is supplied by Γ since (35) represents the forcing function for the disturbance $\partial u / \partial x$. To determine the whole of the energy in the wave it would in general be necessary to solve for the disturbance completely, but in the present case the only other contribution comes from $\text{div } \mathbf{v}$. The forcing function for Δ is found to be for the point source (for a source of length scale l the same modifications as before apply)

$$f = \frac{qa_0^2}{\rho_0} \nabla^2 \left(a_1^2 \frac{\partial^2}{\partial x^2} + \omega^2 \right) \delta(x) \delta(y) \delta(z) \quad (46)$$

and by (32)

$$F = \frac{1}{8\pi^3} \frac{a_0^2 q}{\rho_0} k^2 (a_1^2 k_1^2 - \omega^2) \quad (47)$$

which becomes on the surface $G_1 = 0$

$$F = -\frac{q\omega^4(\alpha^2 - \epsilon)}{8\pi^3 \rho_0 (\alpha^2 - 1 - \epsilon)} \quad (48)$$

and the energy ratio

$$\mathcal{E}_m/\mathcal{E}_s = O(\epsilon^6) \quad (49)$$

or 10^{-30} in the laboratory. The implication of the fact that \mathcal{E}_m is much greater for the Δ component than the Γ component is that for the m.h.d. wave the fluid particles are displaced almost entirely normal to the magnetic field, a result which accords with expectations since propagation along the field lines takes the form of transverse Alfvén motion very nearly. By contrast in the much more powerful near-sound wave the solution for Δ is very nearly the same as for Γ , the difference being the extra α^2 in the numerator for Γ which is a factor between 1 and $1 + \epsilon$; thus $\partial u/\partial x$ is much larger in magnitude than $\partial v/\partial y + \partial w/\partial z$ and is of opposite sign.

The analysis of this section has been given for the sake of completeness. It shows that for all practical purposes under the laboratory conditions of § 2.1 waves of very low frequency from a localized source will propagate only along the magnetic field lines and will closely resemble ordinary sound waves. Physically one may think of the plasma as being very stiff magnetically and very flexible gas-dynamically so that all the energy goes into the gas-dynamics.

2.4. *Wave propagation at frequencies of the order of the ion cyclotron frequency*

Lighthill (1960) discussed this case only in the incompressible limit ($\epsilon \rightarrow \infty$) and his expression for G can be recovered from (28) by noting that, in the context of large a_0 , α^2 and θ^2 are each of order ϵ and by retaining the terms of $O(\epsilon^4)$. The laboratory conditions of current interest, however, correspond with $\epsilon \ll 1$ and with α , θ and χ all of order unity. If the terms in ϵ^3 and ϵ^2 are neglected on the right of (28) the wave number surface may be defined by

$$G_1 \equiv \alpha^2 - 1 + \chi(1 - \alpha^2 - \theta^2) = 0, \quad (50)$$

where the simple factors in (28) have been discarded. The form of the surface is shown in figure 2 for various values of χ . In the low frequency limit, $\chi = 0$, the waves propagate only along the magnetic field at the sound speed and the surface is the plane $\alpha = 1$. As χ increases the surface becomes distorted into a hyperboloid of revolution of which the asymptotes are a cone whose semi-angle reduces with increasing χ until the singular condition is reached at $\chi = 1$ when the surface degenerates to the line $\theta = 0$. During the same range of χ the energy in the wave is also propagated within a cone comprising the envelope of the normals to the wave number surface. The semi-angle of this propagation cone therefore increases with χ and reaches 90° at $\chi = 1$ as shown in figure 3. For values of χ greater than unity the hyperboloid becomes an ellipsoid with major axis joining the points $(\alpha, \theta) = (1, 0)$ and $(-1, 0)$, and whose eccentricity reduces with increasing χ approaching a sphere as $\chi \rightarrow \infty$.

As noted in § 2.3 the amplitude of the wave motion depends very much on the nature of the forcing function. For the case of a disturbance near the origin as given by (37) the forcing function for the disturbance Δ where G has the form (25) is given by

$$f = a_0^2 \left[\frac{\partial^2}{\partial t^2} \left(-\frac{\partial^2}{\partial t^2} + 2a_1^2 \frac{\partial^2}{\partial x^2} \right) \nabla^2 - \frac{m_i^2 a_1^2}{e^2 \mu \rho_0} \frac{\partial^2}{\partial t^2} \frac{\partial^2}{\partial x^2} \nabla^4 - a_1^4 \frac{\partial^4}{\partial x^4} \nabla^2 \right] f_1 e^{i\omega t}, \quad (51)$$

here

$$f_1 = \frac{q \exp \{ -(x^2 + y^2 + z^2)/l^2 \}}{\rho_0 (l\sqrt{\pi})^3} \quad (52)$$

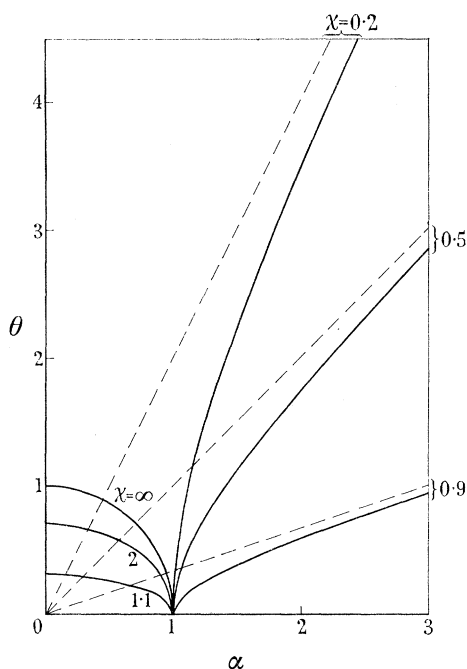


FIGURE 2. Wave number surface for various values of $\chi (a_1 \rightarrow \infty)$. Asymptotes shown dashed. $\chi = (\omega/\omega_i)^2$; $\alpha = k_1 a_0/\omega$; $\theta = (a_0/\omega)\sqrt{(k_2^2 + k_3^2)}$ (\mathbf{k} is wave number vector).

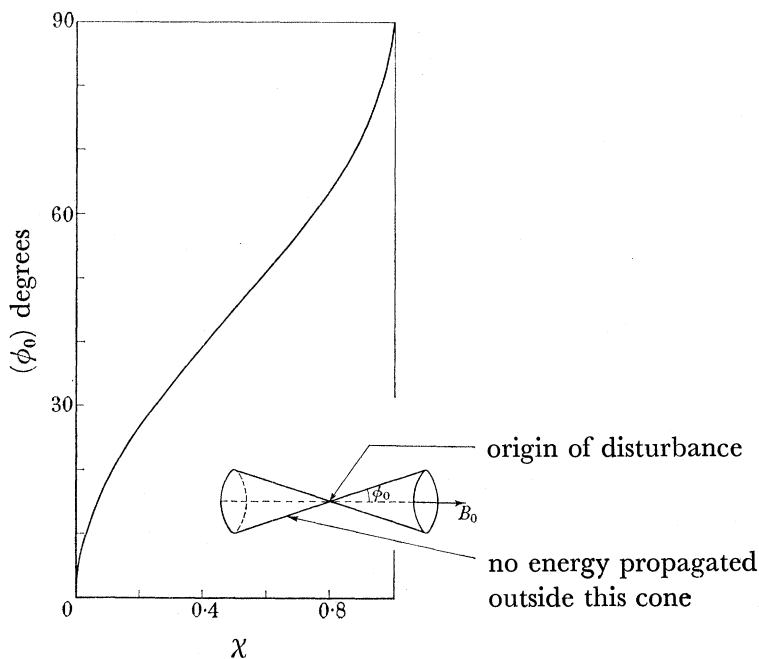


FIGURE 3. Variation of semi-angle of propagation cone with χ . Inset, illustration of conical propagation.

and for Γ the forcing function is

$$f = \frac{a_0^2}{\rho_0} \left[\frac{\partial^2}{\partial t^2} \left\{ -\frac{\partial^2}{\partial t^2} + a_1^2 \left(\frac{\partial^2}{\partial x^2} + \nabla^2 \right) \right\} \frac{\partial^2}{\partial x^2} - \frac{m_i^2 a_1^2}{e^2 \mu \rho_0} \frac{\partial^2}{\partial t^2} \frac{\partial^4}{\partial x^4} \nabla^2 - a_1^4 \frac{\partial^4}{\partial x^4} \nabla^2 \right] f_1 e^{i\omega t}. \quad (53)$$

Equations (51) and (52) are obtained by using (37) on the right-hand side of (15) in the derivation of (23) for Δ and Γ respectively. To determine the corresponding values of F it

is easy to show that

$$\int_{-\infty}^{\infty} \int_{-\infty}^{\infty} \int_{-\infty}^{\infty} \exp[-i(k_1 x + k_2 y + k_3 z)] \left(\frac{\partial}{\partial x}\right)^{2n} f_1 dx dy dz = (-1)^n \frac{q k_1^{2n}}{\rho_0} e^{-\frac{1}{4} l^2 k^2} \quad (54)$$

and that

$$\int_{-\infty}^{\infty} \int_{-\infty}^{\infty} \int_{-\infty}^{\infty} \exp[-i(k_1 x + k_2 y + k_3 z)] \nabla^{2n} f_1 dx dy dz = (-1)^n \frac{q k^{2n}}{\rho_0} e^{-\frac{1}{4} l^2 k^2}. \quad (55)$$

Using these results in equation (32) with f given by (51) and (53) and making the substitutions (26) and (27) leads to, for Δ

$$F = \frac{1}{8\pi^3} \frac{q \omega^6}{\rho \epsilon^2} e^{-\frac{1}{4} l^2 k^2} (\theta^2 + \alpha^2) [\epsilon^2 - 2\alpha^2 \epsilon - \chi \alpha^2 (\theta^2 + \alpha^2) + \alpha^4] \quad (56)$$

and for Γ

$$F = \frac{1}{8\pi^3} \frac{q \omega^6}{\rho_0 \epsilon^2} e^{-\frac{1}{4} l^2 k^2} \alpha^2 [\epsilon^2 - (2\alpha^2 + \theta^2) \epsilon - \chi \alpha^2 (\alpha^2 + \theta^2) + \alpha^2 (\alpha^2 + \theta^2)]. \quad (57)$$

That these are compatible in order of magnitude with the expression for G in (28) can be seen by noting that the coefficient of G in (28) is ϵ^3/ω^6 .

In the context of the laboratory experiment, in which ϵ is very small, the terms in ϵ^2 and ϵ within the square brackets of (56) and (57) may be neglected, and in order to avoid the added complications that arise if the finite size of the disturbance is taken into account a point disturbance will first be assumed so that the exponential factors in (56) and (57) become unity. For large values of k , however, this will not be true and it should be remembered that such regions of the wave number surface will contribute little to the energy of propagation. In practice the finite size of the disturbance is likely to be important; e.g.

$$\exp\left(-\frac{1}{4} l^2 k^2\right) \equiv \exp\left\{-\frac{\omega^2 l^2}{4a_0^2} (\alpha^2 + \theta^2)\right\} \quad (58)$$

and if ω and a_0 are taken as 10^6 rad/sec and 10^3 m/sec respectively (see §2.1) then for $l = 2 \times 10^{-3}$ m (58) becomes $\exp\{-(\alpha^2 + \theta^2)\}$ which cannot be assumed equal to unity without introducing significant errors.

When only the lowest order terms in ϵ are retained the differential equation (23) simplifies and in particular the operator $\partial^2/\partial x^2 \nabla^2$ is common to all terms, both on the left-hand side (equation (23)) and on the right-hand side (equation (51)). This operator may be cancelled since a function ϕ satisfying $\partial^2/\partial x^2 \nabla^2 \phi = 0$ would simply represent another forcing function additional to the one of interest described by $f_1 e^{i\omega t}$. This cancellation is equivalent to cancelling the factor $\alpha^2(\alpha^2 + \theta^2)$ from both G and F whence G may assume the form G_1 in (50) and F , using (56) becomes (ignoring the factor $q/8\pi^3 \rho_0$ since only relative amplitudes matter)

$$F_1 = e^{-\frac{1}{4} l^2 k^2} \{\alpha^2 - \chi(\alpha^2 + \theta^2)\}, \quad (59)$$

or in the limit $kl \rightarrow 0$

$$F_1 = \alpha^2 - \chi(\alpha^2 + \theta^2). \quad (60)$$

To compare the wave amplitude at different frequencies and wave numbers we may define a non-dimensional amplitude function \hat{u} given by

$$\hat{u} = \frac{2|F_1|}{|\nabla G_1| \sqrt{|K(G_1)|}}. \quad (61)$$

With (50) and (60) this gives for propagation of Δ , with the use of (44),

$$\hat{u} = \frac{1}{\chi} \{ |(1-\chi)(\alpha^2 - \chi)| \}^{\frac{1}{2}} \quad (62)$$

on the surface $G_1 = 0$.

The amplitude function \hat{u} given by equation (62) is plotted against α in figures 5 and 6 for various values of χ less than one and greater than one respectively. When $\chi < 1$ the curves are drawn for $\alpha > 1$ only since in this range of χ the wave number surface has no branch in the range $|\alpha| < 1$, and conversely for $\chi > 1$ the curves are drawn for $\alpha < 1$ only. To determine the relative amplitude for waves propagating at some angle ϕ to the direction of magnetic field it is necessary first to find the value of α for which the chosen direction is normal to the wave number surface, and then the appropriate value of \hat{u} is given for this α from figures 5 and 6. The required value of α can be found from figure 4 on which is plotted the direction of the normal to the wave number surface (relative to the magnetic field) against α , given by

$$\tan \phi = \frac{-1}{(\partial\theta/\partial\alpha)_{G_1=0}}, \quad (63)$$

although in view of the symmetry it is sufficient to disregard the sign in (63) and take ϕ to be a positive angle less than 90° , as has been done in figure 4.

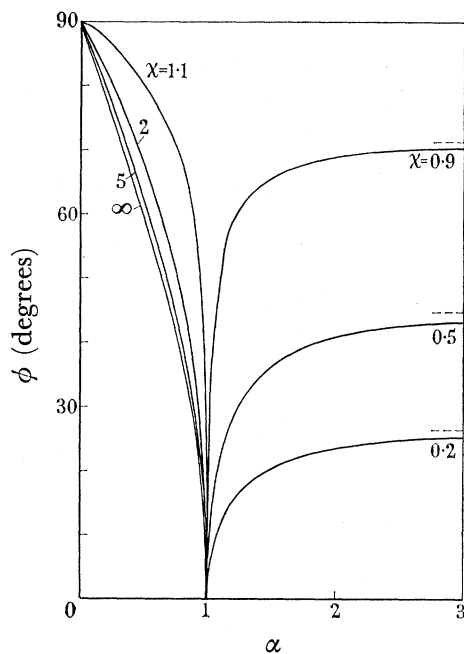


FIGURE 4

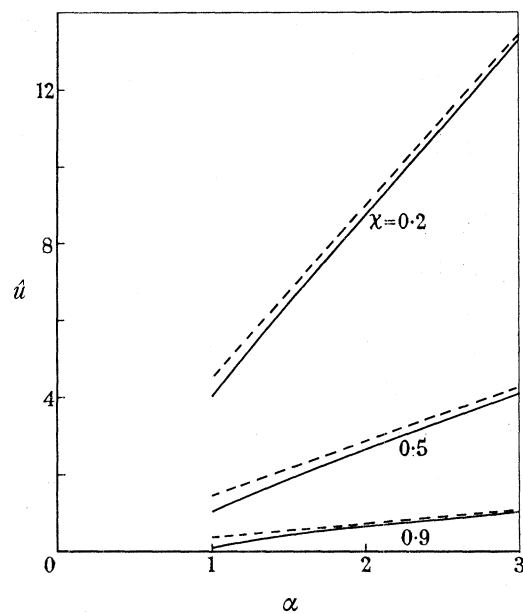


FIGURE 5

FIGURE 4. α on the wave number surface for different directions of propagation relative to the magnetic field (ϕ).

FIGURE 5. Variation of amplitude with α ($\chi < 1$) for point source. Asymptotes are shown dashed. The wave number surface is confined to $|\alpha| > 1$ for $\chi < 1$.

The most interesting range of χ is that between 0 and 1. In this range propagation only takes place for $\phi < \phi_0$, say, where ϕ_0 is the half angle of the propagation cone (figure 3) and increases to 90° as χ increases to one according to $\tan \phi_0 = \pm \sqrt{\chi/(1-\chi)}$. For given χ , less

than one, the amplitude \hat{u} increases with α and becomes indefinitely large as ϕ approaches ϕ_0 which corresponds with the asymptotes on figures 2, 4 and 5. In fact the asymptotic part of figure 2, which represents the conical part of the wave number surface, is specifically excluded from Lighthill's theorem (equations (30) to (32)), since the Gaussian curvature K

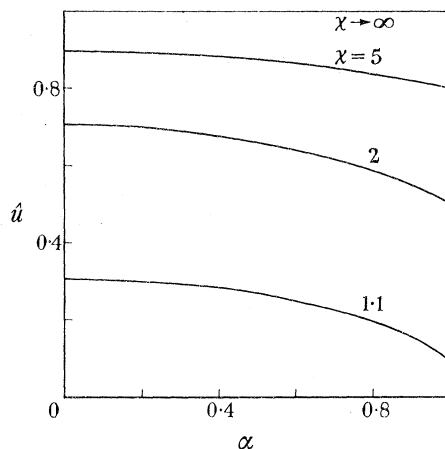


FIGURE 6. Variation of amplitude with α ($\chi > 1$) for point source. The wave number surface is confined to $|\alpha| < 1$ for $\chi > 1$.

is zero there, and what happens is that u instead of behaving like r^{-1} behaves like $r^{-\frac{1}{2}}$ for this region of the surface (Lighthill 1960). The implication is that for large r the amplitude distribution in the wave at a fixed distance from the point source measured along the magnetic field lines, would be zero outside a circle of radius $r \tan \phi_0$, would be large just inside the circle and would diminish rapidly at first and then more slowly towards the centre of the circle.

For $\chi > 1$ the amplitude increases with χ from zero at $\chi = 1$ to $\hat{u} = 1$ at $\chi \rightarrow \infty$, and is spread fairly evenly in all directions, although the amplitude in directions nearly normal to the field is always greater than in directions along the field.

These results for the point source, and particularly those for $\chi < 1$, are greatly modified for practical source sizes. The amplitude then takes the form

$$\hat{u} = \frac{\{(1-\chi)(\alpha^2-\chi)\}^{\frac{1}{2}}}{\chi} \exp\left\{-\frac{\lambda^2(\alpha^2-1+\chi)}{\chi}\right\}, \quad (64)$$

where
$$\lambda^2 = \frac{\omega^2 l^2}{4a_0^2} \quad (65)$$

so that λ is a non-dimensional source radius. The influence of the exponential term is to cut out the contribution to \hat{u} from that part of the wave number surface where α is large, which is just the part that contributes most (for $\chi < 1$) in the case of the point source. The effect is shown for $\lambda = 0.5$ in figures 7 and 8.

If figure 7, where $\lambda = 0.5$, is compared with figure 5, where $\lambda = 0$, it is seen that for small χ the amplitude falls away steadily with increasing α instead of growing, and that for α greater than about 2.5 it is vanishingly small. The implication is that as the wave beam crosses a plane normal to the magnetic field, the illumination from the finite source is

greatest near the centre and becomes vanishingly small at about 0.9 of the limiting radius $r \tan \phi_0$. The contrast between propagation from a point source and a finite source ($\lambda = 0.2$ and $\lambda = 0.5$) is illustrated in figure 9 where \hat{u} is plotted against $\tan \phi / \tan \phi_0$ at a fixed distance from the source. The ratio $\tan \phi / \tan \phi_0$ gives a measure of the distance from the axis

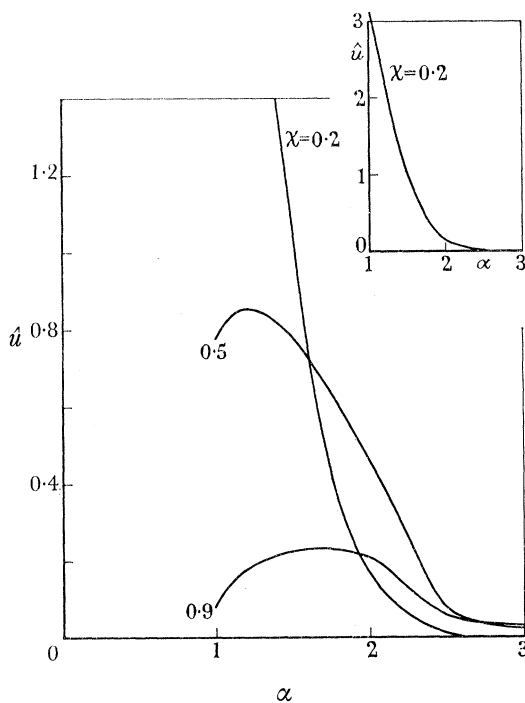


FIGURE 7

FIGURE 7. Variation of amplitude with α ($\chi < 1$) for source $\lambda = 0.5$.

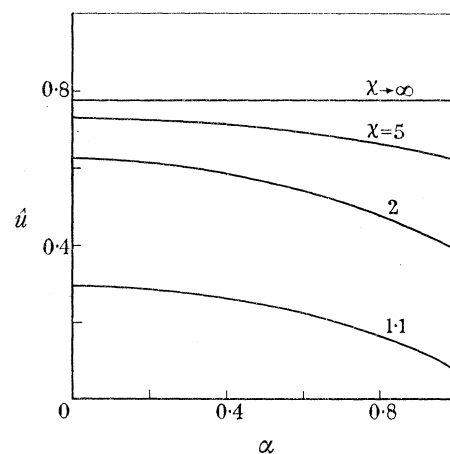


FIGURE 8

FIGURE 8. Variation of amplitude with α ($\chi > 1$) for source $\lambda = 0.5$.

of symmetry, and since the radius vector r from the source to the point of measurement is assumed fixed the amplitude \hat{u} plotted on figure 9 is that appropriate to a sphere with centre at the source: it is as though the wave beam were allowed to illuminate the inner surface of such a sphere. As χ increases from 0.2 to 0.5 to 0.9 for $\lambda = 0.5$ the maximum intensity of illumination moves outwards from the axis of the beam towards the limit of illumination where $\tan \phi = \tan \phi_0$ although the amplitude always falls to zero by the time the limit is reached. The peak amplitude may be found from differentiation of (64) which yields the result that the direction ϕ for which the wave amplitude is a maximum is given by $\phi(\alpha_1)$ from figure 4, where

$$\alpha_1^2 = \chi \left(\frac{1}{2\lambda^2} + 1 \right) \quad \text{or } 1 \text{ whichever is the greater.} \quad (66)$$

Evidently the point source, $\lambda \rightarrow 0$, has $\alpha_1 \rightarrow \infty$ as expected.

The variation of amplitude over a plane normal to the magnetic field may be seen from a plot of $\hat{u} \cos \phi$ against the ratio $\tan \phi / \tan \phi_0$, since on such a plane the factor r^{-1} in the wave amplitude as given by equation (30) is proportional to $\cos \phi$. The result is shown in figure 10. The $\cos \phi$ factor increases in importance as χ approaches unity and has the effect of reducing the amplitude peak for $\chi = 0.9$, $\lambda = 0.5$ so that the amplitude remains nearly constant out

to 80 % of the limiting radius of the beam and then falls to zero at the limiting radius. The amplitude distribution (figures 9 and 10) for the smallest finite source considered ($\lambda = 0.2$) follows that for the point source fairly closely near the centre of the beam before passing through the maximum (66) and falling to zero at $\tan \phi / \tan \phi_0 = 1.0$. The maximum becomes sharper with increasing χ .

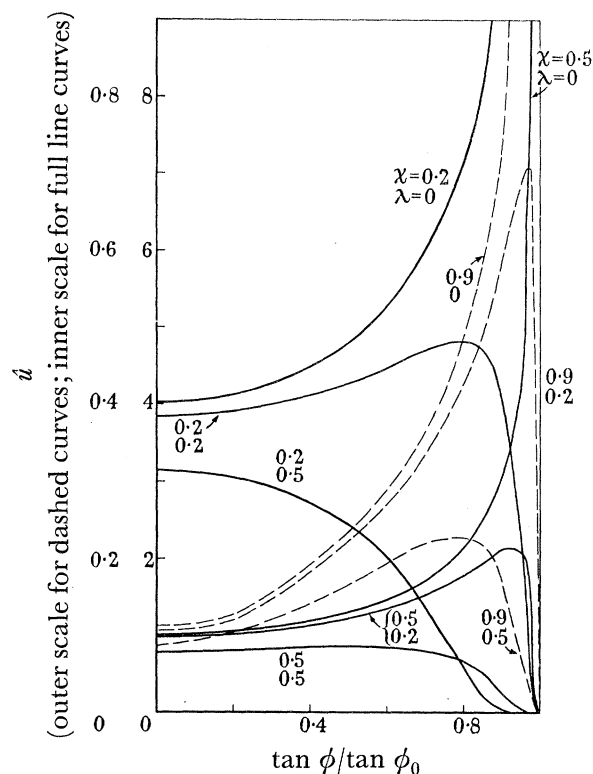


FIGURE 9

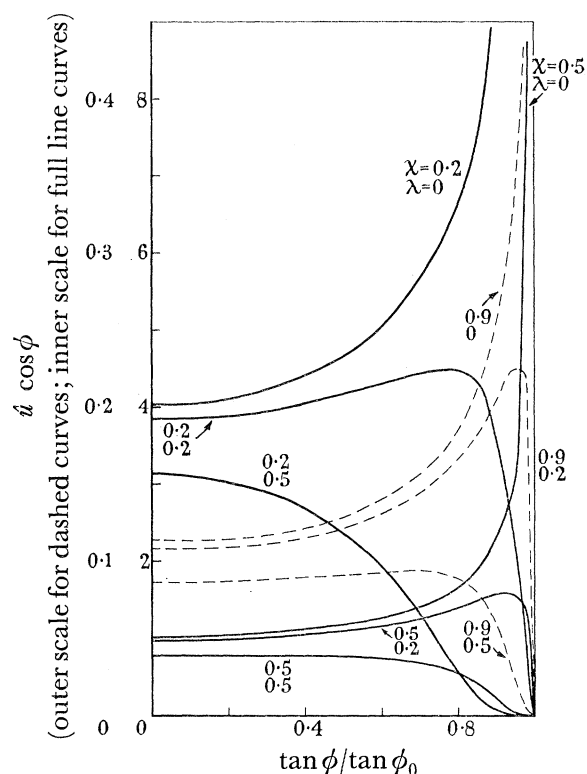


FIGURE 10

FIGURE 9. Variation of amplitude with distance from the axis at a fixed distance from the source.

FIGURE 10. Variation of amplitude with distance from the axis on a plane normal to the magnetic field.

For $\chi > 1$ propagation takes place in all directions, but as the size of the source increases the amplitude near $\alpha = 1$ becomes relatively small, particularly for the smaller values of χ . As $\chi \rightarrow \infty$ the waves spread evenly in all directions for all values of λ , a result which is physically understandable since $\chi \rightarrow \infty$ implies $\omega \rightarrow \infty$ when the reactance of the plasma becomes purely inertial in character (inductive) and the inertia distribution is isotropic.

The results are summarized in table 1.

2.5. The effect of a doublet disturbance at the origin

It has been assumed that the disturbance at the origin takes the form of a fluctuating source of plasma, something like a small pulsating sphere. Other types of disturbance are possible, and in fact more likely in a real experiment. We may first examine the effect of a doublet. This could be considered as the combination of a source at the point (sn_1, sn_2, sn_3) and a sink at the origin so that \mathbf{n} gives the doublet direction and s is very small. The forcing

function is then

$$q e^{i\omega t} \{ \delta(x - sn_1) \delta(y - sn_2) \delta(z - sn_3) - \delta(x) \delta(y) \delta(z) \}$$

which leads to a factor $(e^{-i\mathbf{s}\cdot\mathbf{k}\cdot\mathbf{n}} - 1)$ being applied to the function F for the point source $q e^{i\omega t} \delta(x) \delta(y) \delta(z)$. Since s is very small this is equivalent to a factor $(-i\mathbf{s}\cdot\mathbf{k}\cdot\mathbf{n})$, or for the amplitude factor \hat{u} we may take

$$\hat{u}_d = \hat{u}_p(\mathbf{k}\cdot\mathbf{n})s, \quad (67)$$

where

\hat{u}_d is the doublet amplitude,

\hat{u}_p is the point source amplitude.

TABLE I

$\chi < 1$	$\chi > 1$
(1) A limiting cone of half-angle ϕ_0 , apex at the source and axis along the magnetic field can be defined such that if waves propagate at an angle ϕ to the field, no waves exist for $\phi > \phi_0$	(1) Waves propagate in all directions
(2) ϕ_0 increases from 0 to 90° as χ increases from 0 to 1	(2) The amplitude \hat{u} increases from zero when $\chi = 1$ to some value constant with respect to α and ϕ as $\chi \rightarrow \infty$
(3) The amplitude \hat{u} decreases to zero as $\chi \rightarrow 1$	(3) For a point source, $\lambda = 0$, the increase of amplitude with χ is monotonic but for $\lambda > 0$ the amplitude in some directions may pass through a maximum for some χ , $1 < \chi < \infty$
(4) A point source, $\lambda = 0$, gives peak amplitude just inside the limiting cone, $\phi \rightarrow \phi_0$	(4) For relatively large λ and small χ , waves propagating along the field have a much smaller amplitude than those propagating across the field
(5) A finite source, $\lambda > 0$, gives $\hat{u} \rightarrow 0$ as $\phi \rightarrow \phi_0$. Peak amplitude occurs at the beam centre for small χ and large λ , but for sufficiently small λ it occurs for some ϕ such that $0 < \phi < \phi_0$	

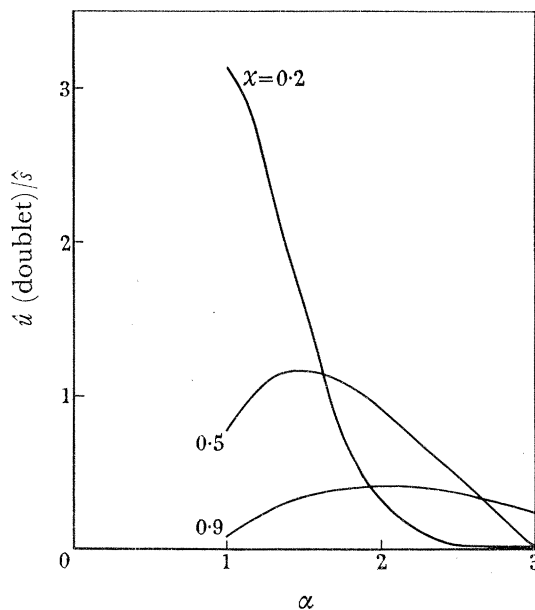


FIGURE 11

FIGURE 11. Variation of amplitude with α ($\chi < 1$) for doublet $\lambda = 0.5$.

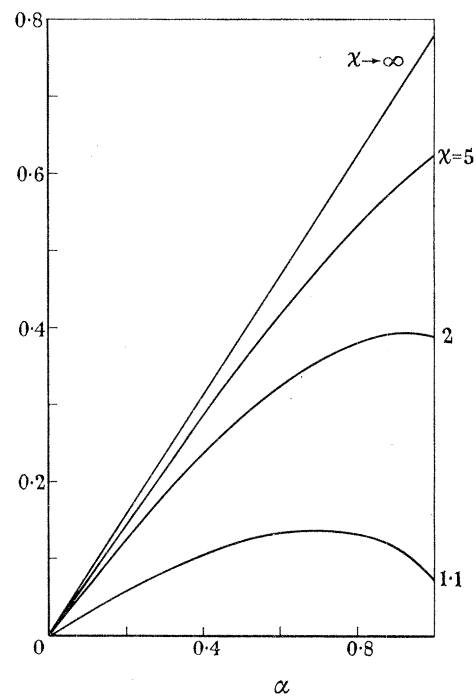


FIGURE 12

FIGURE 12. Variation of amplitude with α ($\chi > 1$) for doublet $\lambda = 0.5$.

The same conversion factor $(\mathbf{k} \cdot \mathbf{n})s$ holds even if the doublet is smeared over a length scale l in the manner of (37). In the particular case where the doublet points in the direction of the magnetic field (67) becomes

$$\left. \begin{aligned} \dot{u}_d &= \dot{u}_p \alpha s, \\ s &= \omega s / a_0. \end{aligned} \right\} \quad (68)$$

where

The non-dimensional parameter s is effectively a non-dimensional frequency in a given experiment of varying frequency but constant doublet strength. For given s the effect on the graphs of \dot{u} so far discussed is that the ordinate must be multiplied by α : this has been done for figures 7 and 8 (i.e. $\lambda = 0.5$) and the result plotted in figures 11 and 12.

The effect of disturbances of a different kind, and in particular a disturbance of the electrons near the origin, is more conveniently treated in §3.

3. TWO-FLUID TREATMENT

3.1. Derivation of the wave number surface

Equations (5) and (6) are used separately, instead of after addition to form a single plasma equation. The advantage is that electron inertia effects can be included if desired and also that it is easier to treat certain types of forcing function. For example a local electrical disturbance will mainly drive the electrons in the first instance so that such a disturbance can be simulated by a source or doublet in the electron fluid only.

The linearized equations are:

$$\text{Continuity} \quad \partial n_e / \partial t + n \operatorname{div} \mathbf{v}_e = f_e e^{i\omega t}, \quad (69)$$

$$\partial n_i / \partial t + n \operatorname{div} \mathbf{v}_i = f_i e^{i\omega t}, \quad (70)$$

where forcing functions have been included, and analogous to (37) would take the form

$$f_e = \frac{N \exp\{-(x^2 + y^2 + z^2)/l^2\}}{(l\sqrt{\pi})^3} \quad (71)$$

and similarly for f_i where N is the total number of electrons or ions produced per second over the length scale l . In (69) and (70) it is assumed that the electron and ion densities are respectively $n + n_e$ and $n + n_i$ where n_e and n_i are the perturbation quantities.

Momentum

$$m_e n \frac{\partial \mathbf{v}_e}{\partial t} + \gamma_e k_B T_e \nabla n_e + en(\mathbf{E} - \mathbf{B}_0 \wedge \mathbf{v}_e) = 0, \quad (72)$$

$$m_i n \frac{\partial \mathbf{v}_i}{\partial t} + \gamma_i k_B T_i \nabla n_i - en(\mathbf{E} - \mathbf{B}_0 \wedge \mathbf{v}_i) = 0, \quad (73)$$

where it is assumed that

$$\nabla p_e = \gamma_e k_B T_e \nabla n_e \quad (74)$$

and similarly for ∇p_i . From Maxwell's equations, where $\mathbf{B} = \mathbf{B}_0 + \mathbf{B}_1$ and \mathbf{B}_1 is the perturbation quantity we can obtain another relation between \mathbf{E} and the fluid velocities

$$\operatorname{curl} \mathbf{E} = -\frac{\partial \mathbf{B}_1}{\partial t}; \quad \operatorname{curl} \mathbf{B}_1 = \mu \mathbf{j} = \mu en(\mathbf{v}_i - \mathbf{v}_e),$$

whence

$$\text{curl curl } \mathbf{E} = -\mu en \left(\frac{\partial \mathbf{v}_i}{\partial t} - \frac{\partial \mathbf{v}_e}{\partial t} \right). \quad (75)$$

Following Allis *et al.* (1963) we shall use matrix equations for the vector quantities but instead of immediately assuming perturbations of the form $\exp \{i(\omega t - k_1 x - k_2 y - k_3 z)\}$ as they do, we shall retain the differential operators leading to an equation such as (4). The following differential operators are defined

$$D_t \equiv \frac{\partial}{\partial t}, \quad (76)$$

a scalar operator, usually associated with the unit matrix;

$$D_g \equiv \begin{bmatrix} \partial/\partial x \\ \partial/\partial y \\ \partial/\partial z \end{bmatrix}, \quad \text{the grad operator;} \quad (77)$$

$$D_d \equiv [\partial/\partial x, \partial/\partial y, \partial/\partial z], \quad \text{the div operator;} \quad (78)$$

$$D_\lambda \equiv \begin{bmatrix} 0 & -\frac{\partial}{\partial z} & \frac{\partial}{\partial y} \\ \frac{\partial}{\partial z} & 0 & -\frac{\partial}{\partial x} \\ -\frac{\partial}{\partial y} & \frac{\partial}{\partial x} & 0 \end{bmatrix}, \quad \text{the curl operator.} \quad (79)$$

Also define I_a as the antisymmetric matrix

$$I_a = \begin{bmatrix} 0 & 0 & 0 \\ 0 & 0 & -1 \\ 0 & 1 & 0 \end{bmatrix} \quad (80)$$

which is used in association with cross-products of \mathbf{B}_0 and \mathbf{B}_0 is taken to be in the x direction. Elimination of n_e and n_i from (69), (70), (72) and (73) then gives

$$\mathbf{v}_e = -enD_e^{-1} D_t \mathbf{E} - \gamma_e k_B T_e D_e^{-1} D_g f_e e^{i\omega t} \quad (81)$$

and

$$\mathbf{v}_i = enD_i^{-1} D_t \mathbf{E} - \gamma_i k_B T_i D_i^{-1} D_g f_i e^{i\omega t}, \quad (82)$$

where we have defined

$$D_e = m_e n D_i^2 - \gamma_e k_B T_e n D_g D_d - en B_0 I_a D_t, \quad (83)$$

$$D_i = m_i n D_i^2 - \gamma_i k_B T_i n D_g D_d + en B_0 I_a D_t. \quad (84)$$

Finally, use of (81) and (82) in (75) gives

$$\{D_\lambda^2 + \mu e^2 n^2 D_t^2 (D_i^{-1} + D_e^{-1})\} \mathbf{E} = \mu en k_B D_t (\gamma_i T_i D_i^{-1} D_g f_i - \gamma_e T_e D_e^{-1} D_g f_e) e^{i\omega t}. \quad (85)$$

Equation (85) is a generalization of (4) to a vector equation, but if (85) is written

$$A \left(\frac{\partial^2}{\partial t^2}, \frac{\partial^2}{\partial x^2}, \frac{\partial^2}{\partial y^2}, \frac{\partial^2}{\partial z^2} \right) \mathbf{E} = \mathbf{b}, \quad (86)$$

where A is the matrix operating on \mathbf{E} , then the result of eliminating E_2 and E_3 , say, would be

$$|A| E_1 = \mathbf{a}_{1i} \cdot \mathbf{b}, \quad (87)$$

where a_{1i} is the first row of the matrix of cofactors of the elements of A . Thus the wave number surface $G = 0$ is given by

$$|A(-\omega^2, -k_1^2, -k_2^2, -k_3^2)| = 0. \quad (88)$$

To simplify matters a little, we may make use of the axisymmetry to select the y direction such that the vector \mathbf{k} lies in the (x, y) plane. The matrix A in (88) is formed by the addition of three matrices, $A_1 + A_2 + A_3$, say, where

$$A_1 = -k^2 \begin{bmatrix} -\eta^2 & \xi\eta & 0 \\ \xi\eta & -\xi^2 & 0 \\ 0 & 0 & -1 \end{bmatrix} \quad (89)$$

and $(\xi, \eta, 0)$ are the direction cosines of \mathbf{k} ,

$$A_2 = -\mu e^2 n^2 \omega^2 \left(-m_i n \omega^2 + \gamma_i k_B T_i n k^2 \begin{bmatrix} \xi^2 & \xi\eta & 0 \\ \xi\eta & \eta^2 & 0 \\ 0 & 0 & 0 \end{bmatrix} + i\omega e n B_0 I_a \right)^{-1}, \quad (90)$$

$$A_3 = -\mu e^2 n^2 \omega^2 \left(-m_e n \omega^2 + \gamma_e k_B T_e n k^2 \begin{bmatrix} \xi^2 & \xi\eta & 0 \\ \xi\eta & \eta^2 & 0 \\ 0 & 0 & 0 \end{bmatrix} - i\omega e n B_0 I_a \right)^{-1}. \quad (91)$$

The relative importance of the different parts of A_2 and A_3 (which are closely related to τ_i and τ_e respectively (Allis *et al.* 1963)) may be seen by dividing both inside and outside the round brackets by the factor $\mu^2 e^2 n^2 \omega^2 / k^2$, and noting that

$$\left. \begin{aligned} \frac{m_i k^2}{\mu e^2 n} &= \frac{a_1^2 k^2}{\omega^2} \chi, \\ \frac{\gamma_i k_B T_i k^4}{\mu e^2 n \omega^2} &= \frac{a_0^2 k^2}{\omega^2} \frac{a_1^2 k^2}{\omega^2} \chi, \\ \frac{i B_0 k^2}{\mu e n \omega} &= \frac{a_1^2 k^2}{\omega^2} i \sqrt{\chi}. \end{aligned} \right\} \quad (92)$$

In equations (92) a_0 and a_1 are velocities based on the ion gas alone.

From (88) we may take

$$G \equiv |A_1 + A_2 + A_3| \quad (93)$$

and to the same order as (28), the determinant (93) can be evaluated after first letting $m_e \rightarrow 0$ in (91). The result may be written

$$G = k^6 \left[\left(\frac{a_0^2}{a_1^2} (1+s) \right)^3 \left\{ a_0^2 (1+s) - 1 \right\} + \left(\frac{a_0^2 (1+s)}{a_1^2} \right)^2 a_0^2 (1+s) \{ \xi^2 + 1 - 2a_0^2 \xi^2 (1+s) \} \right. \\ \left. + \frac{a_0^2 (1+s)}{a_1^2} \{ a_0^2 (1+s) \}^2 \xi^2 \{ \chi - \chi a_0^2 (1+s) + a_0^2 (1+s) \xi^2 - 1 \} \right] \\ \frac{1}{[\chi(1-a_0^2) - (1-a_0^2 \xi^2)] \chi s a_0^2 \{ a_0^2 (1+s) \}^3 \xi^2}, \quad (94)$$

where

$$a_0^2 = \frac{a_0^2 k^2}{\omega^2}; \quad a_1^2 = \frac{a_1^2 k^2}{\omega^2}; \quad s = \frac{\gamma_e T_e}{\gamma_i T_i}. \quad (95)$$

A significant point is that throughout the numerator, \hat{a}_0^2 is everywhere multiplied by $(1+s)$ which implies that the relevant speed of sound is that based on the sum of the electron and ion partial pressures, exactly as in the single fluid treatment when $\nabla p_e + \nabla p_i$ was taken as ∇p . To compare (94) with (28) it is thus necessary to let

$$\hat{a}_0^2(1+s)/\hat{a}_1^2 = \epsilon, \quad \hat{a}_0^2(1+s) = \alpha^2 + \theta^2 \quad \text{and} \quad \hat{a}_0^2(1+s)\xi^2 = \alpha^2, \quad (96)$$

after which the expression in square brackets in the numerator of (94) becomes identical with the right-hand side of (28).

3.2. Electron inertia and electron forcing functions

It is possible to retain (m_e/m_i) in the expansion for G . If this is done a corrected expression corresponding to (28) is obtained and, neglecting $(m_e/m_i)^2$, there results

$$\begin{aligned} \left(\frac{a_0}{\omega a_1}\right)^6 G &= \epsilon \alpha^2 \{ \alpha^2(\alpha^2 + \theta^2) - \alpha^2 - \theta^2 + \chi(\alpha^2 + \theta^2)(1 - \alpha^2 - \theta^2) \} \\ &+ \epsilon^2 \{ (1 - \alpha^2)(2\alpha^2 + \theta^2) - \alpha^2\theta^2 + (\alpha^2 + \theta^2)\hat{m}[(1+s)(\chi - 1) - (\alpha^2 + \theta^2)\chi + \alpha^2] \} \\ &+ \dots, \end{aligned} \quad (97)$$

where

$$\hat{m} = \frac{m_e}{sm_i} \left(\frac{a_1^2}{a_0^2} \right)_{\text{ion}}. \quad (98)$$

In the laboratory condition of § 2.1, with $T_e = T_i$, $\gamma_i = \frac{5}{3}$, $\gamma_e = 1$, the value of \hat{m} is about 2.1; thus the extra term introduced into the coefficient of ϵ^2 (by comparison with (28)) is certainly not small. On the other hand, with ϵ of order 10^{-5} in the laboratory, it is of more practical interest to use the method for examining different types of disturbance in conditions such that both m_e/m_i and a_0^2/a_1^2 are negligible compared with unity.

If m_e/m_i is neglected it is of interest first to recover the results of § 3 by letting $f_e = f_i$, with each given by (71), and by taking the divergence of equation (82). This gives $\text{div } \mathbf{v}_i$ rather than $\text{div } \mathbf{v}$, but to the extent that m_e is negligible by comparison with m_i , \mathbf{v}_i is indistinguishable from \mathbf{v} , and it has in fact been verified that the two-fluid equations yield a left-hand side and right-hand side identical with (28) and (56) respectively if the relations (96) are used. The matrix A^{-1} is given in the appendix. The actual expression for F that is found by this method, and that corresponds with (56) is

$$F = \frac{N\omega^6 e^{-\frac{1}{2}l^2k^2}}{8\pi^3} \hat{a}_0^2(1+s) \{ 1 - 2\hat{a}_1^2\xi^2 - \hat{a}_1^4\xi^2(\chi - \xi^2) \}. \quad (99)$$

Suppose now that instead of $f_i = f_e$ it is assumed that $f_i = 0$ but that f_e is still given by (71), corresponding with a source term in the electron gas only. An extension of this would be to a doublet in the electron gas which would correspond with a disturbance at the origin comprising an oscillatory shift of the electrons in the doublet direction. This is in fact very much what one might expect to be able to do using electric fields in the laboratory.

With a source in the electron gas only it is found that the resulting expression for F is identical with (99) except that the factor $(1+s)$ is replaced by s , a result which has a simple

physical explanation, and could indeed have been anticipated. At these low frequencies (displacement current neglected) and in the case of a massless electron gas, the field electrons can move instantly to neutralize any electric field that is set up. Actually the electric field is not completely neutralized: a little remains in equation (72) to balance the electron pressure gradient, and this residual electric field acts on the ion gas in (73). In effect the electric field is a very stiff spring trying to maintain overall neutrality and is sufficiently stiff that negligible energy is stored in it and the electron pressure gradient is transmitted directly to the ions. It follows that a source or doublet in the electron gas has the same effect as a source or doublet in the neutral fluid of §2 on the basis that the partial pressure of the electron source is the same as the pressure of the source in the neutral fluid.

4. AN EFFECT OF COLLISIONS (FINITE ELECTRICAL CONDUCTIVITY)

In §3 any momentum exchange between ions and electrons was neglected. Such exchange can be represented by introducing collision frequencies ν_i and ν_e into the momentum equation so that (72) and (73) become

$$m_e n \frac{\partial \mathbf{v}_e}{\partial t} + \nabla p_e + en(\mathbf{E} - \mathbf{B}_0 \wedge \mathbf{v}_e) = -nm_e \nu_e (\mathbf{v}_e - \mathbf{v}_i), \quad (100)$$

$$m_i n \frac{\partial \mathbf{v}_i}{\partial t} + \nabla p_i - en(\mathbf{E} - \mathbf{B}_0 \wedge \mathbf{v}_i) = -nm_i \nu_i (\mathbf{v}_i - \mathbf{v}_e), \quad (101)$$

where

ν_i is the average number of times per second that an ion loses all its momentum (relative to the electron fluid) to electrons through collisions,

ν_e is the corresponding collision frequency for electrons.

The momentum exchange terms on the right-hand side of (100) and (101) are identical with the terms $\pm \mathbf{M}$ in (5) and (6) that were later discarded. There follows

$$m_i \nu_i = m_e \nu_e \quad (102)$$

and approximately (Chapman & Cowling 1952)

$$\nu_i = \left(\frac{2m_e}{m_i}\right)^{\frac{1}{2}} \nu_{ii}, \quad \nu_e = \left(\frac{2m_i}{m_e}\right)^{\frac{1}{2}} \nu_{ii}. \quad (103)$$

In equation (101) the order of magnitude of $nm_i \nu_i \mathbf{v}_i$ compared with $nm_i \partial \mathbf{v}_i / \partial t$ is ν_i / ω which from (103) and §2 is about 4×10^{-3} (of order $\sqrt{(m_e/m_i)}$) and so may be treated as a small quantity such that $(\nu_i / \omega)^2$ may be neglected to the same accuracy as is implied in the neglect of m_e/m_i . In equation (100) the collision term is equal to that in equation (101) and the left-hand side is of the same order of magnitude as the left-hand side of (101) so that again the collision term is small, of order $\sqrt{(m_e/m_i)}$ compared with the dominant terms in the equation. At low frequencies ($\chi \ll 1$) the effect of momentum exchange is quite negligible since $\mathbf{v}_i - \mathbf{v}_e$ is then small. However, as χ increases the constraint imposed on the ions by the magnetic field becomes less and \mathbf{v}_i begins to differ substantially from \mathbf{v}_e so that momentum exchange begins to have an effect. For example a plasma source, with zero ν_e and ν_i , gives for relative values of \mathbf{v}_i and \mathbf{v}_e (if we use the analysis of §3 and retain only the

most significant terms)

$$\mathbf{v}_i \sim \begin{bmatrix} \xi^2(\chi-1) \\ \xi\eta\chi \\ i\xi\eta/\chi \end{bmatrix}, \quad \mathbf{v}_e \sim \begin{bmatrix} \chi-\xi^2 \\ 0 \\ 0 \end{bmatrix} \quad (104)$$

with the limiting case as $\chi \rightarrow 0$

$$\mathbf{v}_i \sim \begin{bmatrix} -\xi^2 \\ 0 \\ 0 \end{bmatrix}, \quad \mathbf{v}_e \sim \begin{bmatrix} -\xi^2 \\ 0 \\ 0 \end{bmatrix}. \quad (105)$$

On the other hand as χ increases the difference between \mathbf{v}_i and \mathbf{v}_e does not introduce significant charge separation, which depends on $\text{div}(\mathbf{v}_i - \mathbf{v}_e)$ and from (104)

$$\text{div} \mathbf{v}_i = \text{div} \mathbf{v}_e \sim \xi(\chi - \xi^2). \quad (106)$$

When collisions are taken into account the wave number surface becomes modified by a small amount. If we take the surface for no collision terms to be given (from (28)) by

$$\alpha^2(\alpha^2 + \theta^2) \{ \chi(1 - \alpha^2 - \theta^2) - 1 + \alpha^2 \} = 0 \quad (107)$$

this becomes with collision terms included and using the method of § 3

$$\begin{aligned} & \alpha^2(\alpha^2 + \theta^2) \{ \chi(1 - \alpha^2 - \theta^2) - 1 + \alpha^2 \} + (i\nu_i/\omega) (\alpha^2 + \theta^2) \\ & \times \chi \{ 2\alpha^2(\alpha^2 + \theta^2) - 2\alpha^2 - \theta^2 \} + (\nu_i/\omega)^2 (\alpha^2 + \theta^2)^2 \chi^2 (1 - \alpha^2 - \theta^2) = 0. \end{aligned} \quad (108)$$

The determinant which leads to this expression is given in the appendix. If terms in $(\nu_i/\omega)^2$, which are of order (m_e/m_i) are neglected we can interpret this as implying a small imaginary part to the wave number surface. To examine this the following change of notation is convenient

$$\left. \begin{array}{l} \text{replace } \alpha^2 \text{ by } \alpha^2(1 + ig), \\ \text{replace } \theta^2 \text{ by } \theta^2(1 + ih) \end{array} \right\} \quad (109)$$

so that α^2 and θ^2 satisfy the same wave number surface as in § 2, but there is an additional imaginary part to be accounted for in the wave motion. We have had

$$\begin{aligned} u & \sim \exp i(k_1 x + k_2 y + k_3 z) \\ & \equiv \exp ik(\xi x + \eta y) \\ & \equiv \exp \left[\frac{ik}{\hat{a}_0 \sqrt{(1+s)}} (\alpha x + \theta y) \right] \end{aligned}$$

which now becomes
$$u \sim \exp \left[\frac{ik(\alpha x + \theta y) - \frac{1}{2}k(\alpha g x + \theta h y)}{\hat{a}_0 \sqrt{(1+s)}} \right]. \quad (110)$$

The real part of the exponential in (110) suggests that the momentum exchange gives rise to a small exponential rate of decay of the waves. Since the energy is propagated along rays from the origin this rate of decay must have the same direction ϕ as the group velocity, i.e. the normal to the real part of the wave number surface; then

$$\tan \phi = \frac{\chi \theta}{\alpha(\chi - 1)} = \frac{h\theta}{g\alpha}. \quad (111)$$

Also from the imaginary part of (108) after making the adjustments (109), we have

$$\alpha^2 g(\chi - 1) - (\alpha^2 - 1)(\chi - 1)h = \left(\frac{\alpha^2 - 1}{\alpha^2}\right) \frac{\nu_i}{\omega} (\chi + 2\alpha^2 - 1). \quad (112)$$

Equations (111) and (112) determine g and h , and the resulting rate of decay can be expressed in terms of distance along the radius vector, with due account taken of the fact that propagation is always outwards from the origin. The result is

$$u \sim \exp \left[-\frac{\zeta}{2} \frac{|\alpha^2 - 1|}{\alpha^2} \frac{(\chi + 2\alpha^2 - 1)}{\sqrt{\{(\chi - \alpha^2)(\chi - 1)\}}} \right], \quad (113)$$

where
$$\zeta = r\nu_i/a_0 \quad (114)$$

and where α has the value given by the wave number surface for a given direction of propagation ϕ .

To confirm that the real part of the exponential is always negative (corresponding with decay of the waves), we can see from (111) and (112) that g is given by

$$g = \frac{(\alpha^2 - 1)(\chi + 2\alpha^2 - 1)\nu_i}{\chi^2(\chi - \alpha^2)\omega} \quad (115)$$

which is always negative. The shape of the wave number surface, however, shows that the x component of group velocity has the same sign as the x component of phase velocity; if we take this to be positive then k_x and α are negative and $k\alpha g x$ in (110) is positive. The relative signs of the y components of phase velocity and group velocity are the same for $\chi > 1$ and opposite for $\chi < 1$, but $k\theta h y$ is positive in either case.

We define R to be

$$R = \left. \frac{|\alpha^2 - 1|(\chi + 2\alpha^2 - 1)}{\alpha^2 \sqrt{\{(\chi - \alpha^2)(\chi - 1)\}}} \right\} \quad (116)$$

such that

$$u \sim e^{-\frac{1}{2} R \zeta}.$$

Large R thus means that the corresponding waves decay relatively quickly. R is plotted against α on figures 13 and 14 for $\chi < 1$ and $\chi > 1$ respectively, and if these diagrams are read in conjunction with figure 2 it can be seen that for $\chi < 1$ the decay is most pronounced for direction of propagation nearest to the limiting cone, and that for $\chi > 1$ the decay is most pronounced for directions of propagation normal to the magnetic field. For all values of χ the exponential decay becomes vanishingly small as the direction of propagation approaches the direction of the magnetic field. A further illustration of this effect is given for $\chi < 1$, i.e. for those values of χ for which there is a finite propagation cone, in figure 15 where R is plotted against $\tan \phi / \tan \phi_0$.

These results show that finite electrical conductivity has the effect of reducing the amplitude of waves propagating near to the limiting cone ($\chi < 1$) or normal to the magnetic field ($\chi > 1$). In particular this means that for $\chi < 1$ where conical propagation takes place, finite electrical conductivity has a similar effect to finite source size and the point source results are accordingly unlikely to be obtainable in the laboratory. The maximum amplitude within the propagation cone ($\chi < 1$) must be expected either to lie along the axis of the

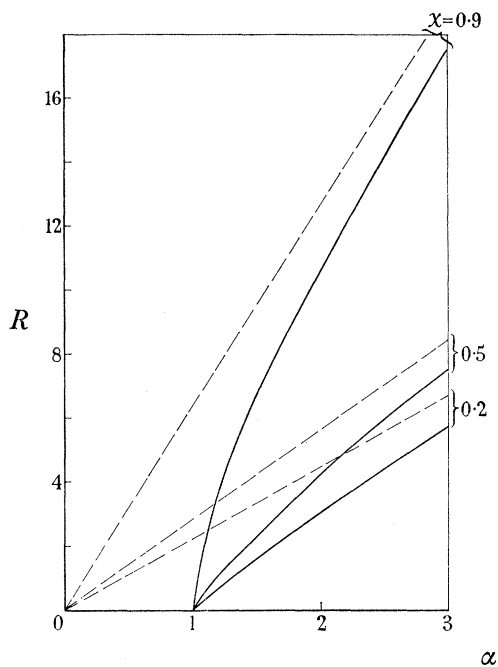


FIGURE 13

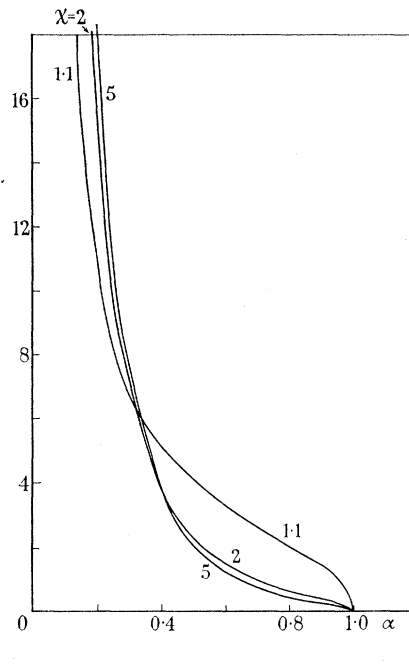


FIGURE 14

FIGURE 13. Wave decay due to imperfect electrical conductivity against α ($\chi < 1$). Wave decays like $e^{-\frac{1}{2}R\zeta}$ where ζ is non-dimensional radius vector from the disturbance. Asymptotes are shown dashed.

FIGURE 14. Wave decay due to imperfect electrical conductivity against α ($\chi > 1$). Wave decays like $e^{-\frac{1}{2}R\zeta}$ where ζ is non-dimensional radius vector from the disturbance.

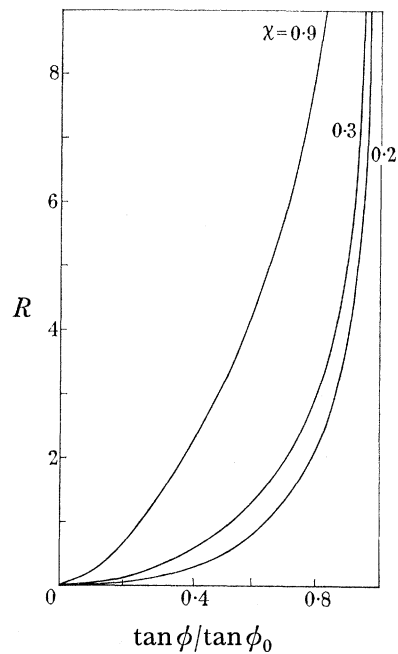


FIGURE 15. Variation in wave decay with propagation angle ($\chi < 1$). Wave decays like $e^{-\frac{1}{2}R\zeta}$.

cone, or to approach the axis of the cone as the distance from the source of the disturbance increases. At sufficiently large distance from the source of the disturbance propagation along the magnetic field (in either direction) will be all that remains of the wave.

5. CONCLUSIONS

The nature of wave propagation from a finite or point source in the presence of a magnetic field such that ω/ω_i ranges from zero through unity to infinity has been indicated in table 1 of § 2.4. In addition it has been shown:

- (1) that a disturbance in the form of a doublet leads to an amplitude factor $(\mathbf{k} \cdot \mathbf{n})$ compared with a simple source, where \mathbf{n} is the direction of the doublet;
- (2) that the effect of changes in electron temperature is fully represented by corresponding changes in the plasma pressure $p = p_e + p_i$;
- (3) that sources in the electron gas have the same effect as sources in the neutral plasma to the extent that m_e/m_i is negligible;
- (4) that finite electron inertia can be allowed for if desired (equations (97) and (98));
- (5) that finite electrical conductivity adds to the equations terms of order $\sqrt{(m_e/m_i)}$ which may be interpreted as introducing a small exponential rate of decay to the waves;
- (6) that this decay is most pronounced for directions ϕ close to ϕ_0 ($\chi < 1$) or close to 90° ($\chi > 1$) and is vanishingly small for $\phi = 0$.

APPENDIX. THE MATRIX A^{-1} (§3) AND THE WAVE NUMBER DETERMINANT (§4)

The matrix $A(-\omega^2, -k_1^2, -k_2^2, -k_3^2)$ from equation (88) may be written

$$A = \frac{k^2}{\hat{a}_1^2 c} \begin{bmatrix} a_1 & d_1 & ie_1 \\ d_1 & b_1 & if_1 \\ -ie_1 & -if_1 & c_1 \end{bmatrix}, \quad (\text{A } 1)$$

where

$$c = \chi(1 - \hat{a}_0^2) - (1 - \hat{a}_0^2 \xi^2) \quad (\text{A } 2)$$

and

$$\left. \begin{aligned} a_1 &= \hat{a}_1^2 c \eta^2 + 1 - \hat{a}_0^2 \eta^2 - \frac{1}{\chi} \left(1 + \frac{c}{\hat{a}_0^2 s \xi^2} \right), \\ b_1 &= \hat{a}_1^2 c \xi^2 + 1 - \hat{a}_0^2 \xi^2, \\ c_1 &= \hat{a}_1^2 c + 1 - \hat{a}_0^2, \\ d_1 &= \xi \eta (-\hat{a}_1^2 c_1 + \hat{a}_0^2), \\ e_1 &= -\frac{\eta}{\xi \sqrt{\chi}} \{ 1 - \chi(1 - \hat{a}_0^2) \}, \\ f_1 &= -\sqrt{\chi(1 - \hat{a}_0^2)}. \end{aligned} \right\} \quad (\text{A } 3)$$

Then

$$A^{-1} = \frac{\hat{a}_1^2 c}{k^2 C} \begin{bmatrix} a_2 & d_2 & ie_2 \\ d_2 & b_2 & if_2 \\ -ie_2 & -if_2 & c_2 \end{bmatrix}, \quad (\text{A } 4)$$

where C is the determinant of the matrix in (A 1) and $a_2 \dots f_2$ are the cofactors of $a_1 \dots f_1$ in

the same matrix. The expressions are

$$\left. \begin{aligned}
 a_2 &= \hat{a}_1^4 c^2 \xi^2 + \hat{a}_1^2 c (1 + \xi^2 - 2\xi^2 \hat{a}_0^2) + (1 - \hat{a}_0^2) (1 - \hat{a}_0^2 \xi^2) - \chi (1 - \hat{a}_0^2)^2, \\
 b_2 &= \hat{a}_1^4 c^2 \eta^2 + \hat{a}_1^2 c \left\{ 1 + \eta^2 (1 - 2\hat{a}_0^2) - \frac{1}{\chi} \left(1 + \frac{c}{\hat{a}_0^2 s \xi^2} \right) \right\} \\
 &\quad - \frac{1}{\chi} \left\{ \left(1 + \frac{c}{\hat{a}_0^2 s \xi^2} \right) (1 - \hat{a}_0^2) + \frac{\eta^2}{\xi^2} \right\} + \frac{2\eta^2}{\xi^2} (1 - \hat{a}_0^2) + (1 - \hat{a}_0^2) (1 - \hat{a}_0^2 \eta^2) \\
 &\quad - \frac{\eta^2}{\xi^2} \chi (1 - \hat{a}_0^2)^2, \\
 c_2 &= \hat{a}_1^2 c \left\{ 1 - \frac{1}{\chi} \left(\xi^2 + \frac{c}{\hat{a}_0^2 s} \right) \right\} + 1 - \hat{a}_0^2 - \frac{1}{\chi} (1 - \hat{a}_0^2 \xi^2) \left(1 + \frac{c}{\hat{a}_0^2 s \xi^2} \right), \\
 d_2 &= \hat{a}_1^4 c^2 \xi \eta + \hat{a}_1^2 c \xi \eta (1 - 2\hat{a}_0^2) + \frac{\eta}{\xi} (1 - \hat{a}_0^2) (1 - \xi^2 \hat{a}_0^2) - \frac{\eta}{\xi} \chi (1 - \hat{a}_0^2)^2, \\
 e_2 &= -\hat{a}_1^2 \frac{c \xi \eta}{\sqrt{\chi}} - \frac{\eta}{\xi \sqrt{\chi}} (1 - \hat{a}_0^2 \xi^2) + \frac{\eta}{\xi} \sqrt{\chi} (1 - \hat{a}_0^2), \\
 f_2 &= -\frac{\hat{a}_1^2 c \eta^2}{\sqrt{\chi}} + \frac{1}{\sqrt{\chi}} \left\{ 1 - \hat{a}_0^2 \xi^2 + \frac{c}{\hat{a}_0^2 s \xi^2} (1 - \hat{a}_0^2) \right\}
 \end{aligned} \right\} \quad (\text{A } 5)$$

$$\text{and} \quad C = c^2 \left[\frac{\hat{a}_1^4}{\chi \hat{a}_0^2 s} \{ \chi (-1 + \hat{a}_0^2 (1 + s)) + 1 - \xi^2 \hat{a}_0^2 (1 + s) \} \right. \\
 \left. + \frac{\hat{a}_1^2}{\chi \hat{a}_0^2 s} \left\{ 2\hat{a}_0^2 (1 + s) - \frac{(1 + \xi^2)}{\xi^2} \right\} + \frac{1}{\chi \hat{a}_0^2 s \xi^2} \{ 1 - \hat{a}_0^2 (1 + s) \} \right]. \quad (\text{A } 6)$$

The determinant which leads to equation (108) is

$$\text{determinant} = |B_1 + B_2|, \quad (\text{A } 7)$$

where B_1 and B_2 are matrices given by

$$B_1 = \begin{bmatrix} -\frac{\hat{\nu}_i \eta^2}{\xi^2} \left[\frac{\xi^2}{c} \{ \chi (1 - \hat{a}_0^2) - 1 \} - \frac{1}{\hat{a}_0^2 s} \right] + \eta^2, & \frac{\hat{\nu}_i \eta}{\xi} \left[\frac{\xi^2}{c} \{ \chi (1 - \hat{a}_0^2) - 1 \} - \frac{1}{\hat{a}_0^2 s} \right] - \xi \eta, & i \hat{\nu}_i \frac{\eta \sqrt{\chi}}{\xi} \left(\frac{\hat{a}_0^2 \xi^2}{c} - 1 \right) \\ \frac{\hat{\nu}_i \chi \xi \eta}{c} (1 - \hat{a}_0^2) - \xi \eta, & -\frac{\hat{\nu}_i \xi^2 \chi}{c} (1 - \hat{a}_0^2) + \xi^2, & i \hat{\nu}_i \sqrt{\chi} \left(\frac{1 - \hat{a}_0^2 \xi^2}{c} + 1 \right) \\ i \hat{\nu}_i \frac{n \sqrt{\chi}}{\xi} \left\{ \frac{\xi^2 (1 - \hat{a}_0^2)}{c} + 1 \right\}, & -i \hat{\nu}_i \sqrt{\chi} \left\{ \frac{\xi^2 (1 - \hat{a}_0^2)}{c} + 1 \right\} & -\frac{\hat{\nu}_i \chi}{c} (1 - \hat{a}_0^2) + 1 \end{bmatrix}, \quad (\text{A } 8)$$

$$B_2 = \frac{1}{\chi \hat{a}_1^2} \begin{bmatrix} \frac{\chi}{c} (1 - \hat{a}_0^2 \eta^2), & \frac{\hat{a}_0^2 \chi \xi \eta}{c} & -\frac{i \sqrt{\chi} \hat{a}_0^2 \xi \eta}{c} + \frac{i \sqrt{\chi} \eta}{\xi} \\ \frac{\chi \hat{a}_0^2 \xi \eta}{c}, & \frac{\chi}{c} (1 - \hat{a}_0^2 \xi^2), & -\frac{i \sqrt{\chi}}{c} (1 - \hat{a}_0^2 \xi^2) - i \sqrt{\chi} \\ \frac{i \sqrt{\chi} \hat{a}_0^2 \xi \eta}{c} - \frac{i \sqrt{\chi} \eta}{\xi}, & \frac{i \sqrt{\chi}}{c} (1 - \hat{a}_0^2 \xi^2) + i \sqrt{\chi}, & \frac{\chi}{c} (1 - \hat{a}_0^2) \end{bmatrix} \quad (\text{A } 9)$$

and where $\hat{\nu}_i = i \nu_i / \omega$.

PRINCIPAL SYMBOLS

symbols	units	explanation
$A; A_1; A_2; A_3$		matrices (see equations (86) to (91))
$\mathbf{B}; \mathbf{B}_0; \mathbf{B}_1$	T	magnetic field; imposed field; perturbation field
$D_i; D_g; D_d; D_\Lambda; D_e; D_i$		operators (see equations (76) to (84))
\mathbf{E}	Vm^{-1}	electric field
$\mathcal{E}_s; \mathcal{E}_m$		relative energies (equation (40))
$F; F_1$		functions of wave number (see equation (32))
$G; G_1$		functions of wave number and frequency (equation (24))
I_a		antisymmetric matrix (equation (80))
K		Gaussian curvature
\mathbf{M}	N m^{-3}	momentum exchange term (equations (5) and (6))
N	s^{-1}	source strength (equation (71))
T	$^\circ\text{K}$	temperature
$a_0; a_1$	m s^{-1}	sound speed; Alfvén speed
$\hat{a}_0; \hat{a}_1$		non-dimensional forms of a_0 and a_1
e	C	electron charge
$f; f_1$		forcing functions
g		see equations (109)
h		see equations (109)
\mathbf{j}	A m^{-2}	electrical current density
\mathbf{k}	m^{-1}	wave number vector ($\mathbf{k} = k_1, k_2, k_3$)
k_B	$\text{J } ^\circ\text{K}^{-1}$	Boltzmann constant
l	m	source size
m	k	particle mass
\hat{m}		mass ratio (equation (98))
\mathbf{n}		doublet direction
$n; n_i; n_e$	m^{-3}	particle density; perturbation values
p	N m^{-2}	pressure
q	k s^{-1}	source strength
\mathbf{r}	m	radius vector
s	m	doublet arm (§ 2.4)
$\hat{s}; s$		non-dimensional doublet arm; temperature ratio (equation (95))
t	s	time
$u; u_g$	m s^{-1}	velocity amplitude; group velocity
$\hat{u}; \hat{u}_d; \hat{u}_p$		non-dimensional amplitudes
\mathbf{v}	m s^{-1}	velocity ($\mathbf{v} = u, v, w$)
$x; y; z$	m	rectangular coordinates
Γ	s^{-1}	$\partial u / \partial x$
α		$k_1 a_0 / \omega$
γ		ratio of specific heats
ϵ		a_0^2 / a_1^2
ζ		rv_i / a_0
η		$(\xi, \eta, 0)$ are the direction cosines of \mathbf{k} in §§ 3 and 4. Also resistivity (equation (7))
θ		$a_0 \sqrt{(k_2^2 + k_3^2)} / \omega$
λ		$\omega l / 2a_0$
μ	$\Omega \text{ s m}^{-1}$	permeability
ν	s^{-1}	collision frequency
ξ		direction cosine (see η)
ρ	k m^{-3}	density
τ	s	collision time
$\phi; \phi_0$		propagation angle relative to magnetic field; semi-angle of propagation cone
χ		$(\omega / \omega_i)^2$
$\omega; \omega_p; \omega_i; \omega_e$	s^{-1}	frequency; plasma frequency; ion cyclotron frequency; electron cyclotron frequency

In general suffix i refers to ions and suffix e to electrons; e.g. p_i and p_e are the partial pressures of the ion and electron gases respectively.

REFERENCES

- Allis, W. P., Buchsbaum, S. J. & Bers, A. 1963 *Waves in anisotropic plasmas*. M.I.T. Press.
- Broadbent, E. G. 1961 A note on a possible experiment on the propagation of longitudinal waves through an ionised gas in the presence of a magnetic field. Unpublished Ministry of Technology Report.
- Chapman, S. & Cowling, T. G. 1952 *The mathematical theory of non-uniform gases*. Cambridge University Press.
- Frood, D. G. H. 1963 *Proc. Sixth Int. Conf. on Ionization Phenomena in Gases, Paris 1963*, **3** SERMA, 107–114.
- Knight, J. 1965 The production of an alkali metal plasma by surface ionization. *R.A.E. Tech. Rep.* 65120.
- Lighthill, M. J. 1960 *Phil. Trans. A* **252**, 397.
- Neubert, H. K. P. 1966 Gaseous plasmas in the laboratory. *R.A.E. Tech. Rep.* 66073.